GIS-BASED SITE SUITABILITY ANALYSIS AND MATHEMATICAL MODELING FOR WIND ENERGY PLANNING: AN INTEGRATED APPROACH

Dr. Selen AVCI AZKESKİN
Prof. Dr. Zerrin ALADAĞ

ISBN 978-625-5753-27-4
Ankara - 2025

GIS-BASED SITE SUITABILITY ANALYSIS AND MATHEMATICAL MODELING FOR WIND ENERGY PLANNING: AN INTEGRATED APPROACH

AUTHORS

Dr. Selen AVCI AZKESKİN[1]

Prof. Dr. Zerrin ALADAĞ[2]

[1] Kocaeli University, Faculty of Engineering, Kocaeli, Türkiye
selen.avci@kocaeli.edu.tr
ORCID ID: 0000-0001-7433-5696

[2] İstanbul Nişantaşı University, Faculty of Engineering and Architecture, İstanbul, Türkiye
zerrin.aladag@nisantasi.edu.tr
ORCID ID: 0000-0002-5986-7210

DOI: https://doi.org/10.5281/zenodo.17812098

Copyright © 2025 by UBAK publishing house
All rights reserved. No part of this publication may be reproduced, distributed or transmitted in any form or by
any means, including photocopying, recording or other electronic or mechanical methods, without the prior written permission of the publisher, except in the case of brief quotations embodied in critical reviews and certain other noncommercial uses permitted by copyright law. UBAK International Academy of Sciences Association Publishing House®
(The Licence Number of Publicator: 2018/42945)

E mail: ubakyayinevi@gmail.com
www.ubakyayinevi.org
It is responsibility of the author to abide by the publishing ethics rules.
UBAK Publishing House – 2025©

ISBN: 978-625-5753-27-4

December / 2025
Ankara / Turkey

PREFACE

The rapid transformation in the global energy landscape has made it imperative for countries to develop sustainable, reliable, and environmentally conscious energy policies. The effective utilization of renewable energy resources not only enhances energy security but also supports economic development, reduces environmental pressures, and contributes to social well-being. Within this context, wind energy stands out as a critical component of Türkiye's energy future due to its high potential, technological maturity, and broad applicability. However, determining the most suitable locations for wind turbines is a complex process that requires the simultaneous consideration of technical, environmental, spatial, and socioeconomic factors.

This book has been prepared to present an integrated framework that combines spatial analysis and mathematical modeling for wind energy planning. By merging Geographic Information Systems (GIS)-based site suitability analyses with a mixed-integer linear programming approach, the study offers a scientific and practical decision-support methodology for wind turbine siting. The case study conducted for the province of Kocaeli enables both the technical assessment of regional potential and the evaluation of the proposed model under real-world conditions. Importantly, the approach presented here is not limited to Kocaeli; it can be readily adapted to other provinces and regions that share similar geographic and technical characteristics.

The primary objective of this book is to serve as a comprehensive reference for academics, researchers, engineers, planners,

policymakers, and energy sector professionals working in the field of renewable energy planning. Developing a holistic approach that guides wind energy investments toward the most suitable areas, minimizes environmental impacts, and enhances economic efficiency has become more crucial than ever. The methodological framework presented in this book aims to provide a solid scientific foundation for addressing these needs.

In preparing this work, extensive national and international literature on renewable energy has been utilized, and a strong interaction between GIS techniques and optimization models has been established. The motivation behind this study has been to contribute to academic knowledge while also offering practical and applicable solutions for real-world energy planning problems.

It is our hope that this book will shed light on the steps to be taken toward achieving Türkiye's sustainable energy goals and contribute to the effective planning of wind energy investments.

04/12/2025

Dr. Selen AVCI AZKESKİN

Prof. Dr. Zerrin ALADAĞ

TABLE OF CONTENTS

GIS-BASED SITE SUITABILITY ANALYSIS AND MATHEMATICAL MODELING FOR WIND ENERGY PLANNING: AN INTEGRATED APPROACH

Dr. Selen AVCI AZKESKİN
Prof. Dr. Zerrin ALADAĞ

INTRODUCTION

The increasing global energy demand, the environmental impacts of fossil fuels, and the risks associated with climate change have urged countries to develop sustainable energy strategies based on renewable resources. Within this transformation, wind energy has become a central component of energy policies owing to its technological maturity, low operating costs, environmental advantages, and growing economic feasibility. However, assessing a region's wind energy potential is not limited to measuring wind speed; it requires the systematic analysis of multidimensional criteria such as land use, environmental constraints, technical suitability, infrastructure accessibility, and social considerations.

In this context, Geographic Information Systems (GIS) provide a powerful decision-support tool for wind turbine siting. GIS-based suitability analyses enable the integrated evaluation of spatial data, allowing complex datasets to be mapped, visualized, and examined through multi-criteria approaches. Nevertheless, determining the

optimal placement of wind turbines within the identified suitable areas necessitates the use of mathematical modeling. Mathematical models offer an effective solution by simultaneously evaluating cost, energy production, environmental constraints, and technical parameters to determine the optimal turbine configuration.

This book develops a holistic approach to wind energy planning by integrating GIS-based site suitability analysis with mathematical modeling. First, spatial and technical criteria used in wind energy planning were identified based on the existing literature, and the province of Kocaeli was selected as the case study area. Kocaeli was chosen primarily due to its industrial intensity, high energy demand, variable wind profiles across coastal and inland zones, and its geographically favorable structure for renewable energy investments. Suitability maps were generated using GIS, followed by the development of a mathematical model designed to optimally locate onshore wind turbines within the identified suitable zones. This integrated approach supports systematic decision-making processes in wind energy investment planning and provides a method that can be applied at the regional level.

The primary aim of this book is to present a scientifically grounded, applicable, and generalizable methodology for decision makers by demonstrating the relationship between spatial analyses and optimization models in wind energy planning. The methods and findings presented here serve as a valuable resource for academics, researchers, energy experts, planners, and public authorities. This

book was developed by expanding a section of Selen AVCI AZKESKİN's doctoral dissertation, numbered 970827.

1. ENERGY AND THE PERSPECTIVE OF SUSTAINABLE ENERGY

Energy is one of the fundamental components of modern societies' economic growth, technological progress, and overall social welfare. All sectors from industrial production to transportation, from digital infrastructure to agriculture require a continuous and reliable supply of energy. Increasing global population, rapid urbanization, and technological transformation drive energy demand higher each year, compelling countries to use existing resources more efficiently while simultaneously developing new energy strategies. Today, energy is not merely a technical necessity; it is a strategic factor that shapes economic stability, national security, environmental sustainability, and international relations.

At the center of contemporary energy discussions lies the concept of sustainable energy. Sustainable energy refers to production and consumption patterns that do not harm the environment, that are economically viable, that safeguard the rights of future generations, and that are socially acceptable. This approach aims not only to meet current demand but also to ensure the long-term resilience of energy systems. Sustainable energy encompasses a broad set of objectives, including the development of renewable energy resources, increasing

energy efficiency, promoting clean technologies, and reducing the carbon footprint within an integrated framework.

Energy resources are generally classified into non-renewable and renewable categories. Non-renewable resources include fossil fuels such as petroleum, natural gas, and coal. Although these resources have formed the backbone of global energy supply for centuries, their combustion leads to significant greenhouse gas emissions and contributes to climate change. The limited nature of fossil fuel reserves also results in price volatility and supply security concerns. In contrast, nuclear energy is a low-carbon alternative to fossil fuels; however, issues related to the safe management of radioactive waste, the potential for nuclear accidents, and public perception of associated risks cause many countries to approach nuclear power cautiously within their energy policies.

Renewable energy resources, on the other hand, are naturally replenished through environmental cycles, do not carry the risk of depletion, and have relatively low environmental impacts. These resources including solar, wind, geothermal, hydroelectric, and biomass energy constitute the foundation of sustainable energy systems. Solar energy has evolved into a rapidly expanding technology with decreasing costs and widespread applicability. Hydroelectric energy remains a stable electricity source, particularly in developing economies. Geothermal energy offers the advantage of continuous, uninterrupted power production, while biomass energy

contributes to waste management and supports local economic development.

Among these resources, wind energy has gained remarkable prominence, especially over the past two decades, as a result of significant technological advancements. Improvements in turbine efficiency, reductions in investment costs, growth in turbine size, and increases in energy yield per unit area have made wind energy a strategic option in the energy policies of many countries. Wind energy is generated by converting the kinetic energy of air movement into mechanical energy through rotor blades and subsequently into electrical energy via a generator. Wind turbines begin producing electricity when wind speeds reach approximately 3 m/s, operate with high efficiency within their optimal range, and shut down during extreme winds for safety. These characteristics make wind energy both an environmentally clean and economically competitive resource.

The real potential of wind energy, however, depends on the accurate identification of suitable locations and the optimal placement of turbines. Wind speed alone is not sufficient; factors such as land use, distance from residential areas, protection of natural habitats, topography, infrastructure accessibility, and various environmental constraints must be assessed together (Avcı Azkeskin & Aladağ, 2025). At this point, scientific tools such as GIS and mathematical modeling become essential, enabling wind energy investments to be planned more safely, economically, and sustainably.

1.1. Wind Energy Potential in Türkiye

Türkiye possesses a significant wind energy potential owing to its geographical position, topographic diversity, and climatic characteristics. The country's three-sided maritime surroundings, extensive mountainous regions in the interior, valleys, elevated plateaus, and coastal landforms shape wind flow patterns in various ways, creating highly favorable atmospheric conditions for wind energy generation. This diversity in topography and climate enables the availability of wind-power-producing areas not only along coastal zones but also across vast inland regions.

As illustrated in Figure 1, Türkiye's national Wind Energy Potential Atlas (REPA) clearly demonstrates that wind speeds do not exhibit a homogeneous distribution across the country.

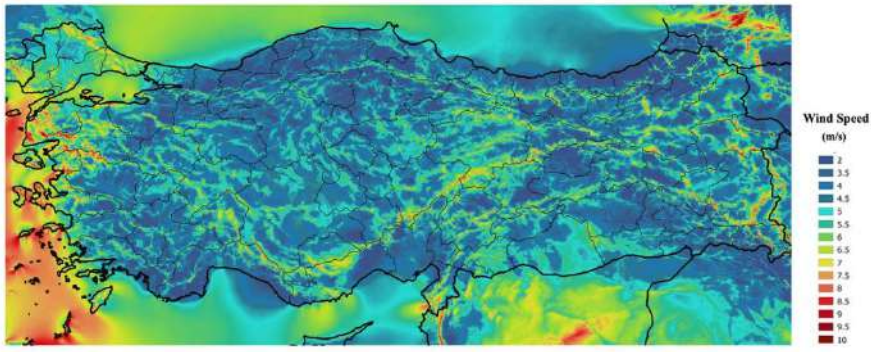

Figure 1: Türkiye Wind Energy Potential Atlas (REPA)
Reference: T.C. Ministry of Energy and Natural Resources, 2024

Coastal regions particularly the Aegean and Marmara coastlines are characterized by relatively high and stable wind speeds throughout the

year. These areas, highlighted in red and yellow tones on the map, represent locations where a substantial portion of Türkiye's wind energy investments are concentrated. The Çanakkale–Balıkesir corridor, the vicinity of İzmir, and the coastal belt of the Marmara Sea rank among the most productive wind corridors in the country. However, Türkiye's wind potential is not limited to its coastal regions. Elevated plateau zones of Central Anatolia, wind-flow corridors extending along valleys, the open and high-altitude areas of Eastern Anatolia, and the inland parts of Thrace exhibit noteworthy potential, represented by the green-to-yellow color transitions on the REPA map. Although wind speeds in these regions are generally lower than those along the coasts, advancements in modern turbine technologies which allow profitable electricity production even at moderate wind speeds have made these inland areas increasingly attractive for investment.

The Black Sea coastline exhibits a more complex wind distribution due to steep topography and dense forest cover; yet the mountain ranges running parallel to the coast create localized strong wind corridors, offering opportunities for micro scale wind energy production. In the Mediterranean region, regular sea land breeze systems observed especially during summer months also provide intermittent but meaningful wind potential in certain localities.

One of the key strengths of Türkiye's wind energy potential lies in the continuity of wind throughout the year and the fact that seasonal variations do not entirely interrupt electricity generation. Achieving high-capacity factors, particularly in the Aegean and Marmara regions,

makes these areas strategic for large-scale wind power plant investments. Moreover, REPA analyses combined with the progress of turbine technologies reveal that new economically viable investment zones are emerging across various parts of the country.

1.2. The Energy Profile of Kocaeli and Its Importance for Wind Energy

Kocaeli is among the provinces with the highest energy demand in Türkiye, largely due to its status as one of the country's most intensive industrial hubs. Geographically connected directly to Istanbul and situated at the center of the Marmara Region's west east industrial corridor, the province plays a pivotal role in Türkiye's economy with its strong production capacity and advanced logistics infrastructure. The concentration of energy-intensive sectors such as automotive, chemicals, metallurgy, energy production, shipbuilding, and machinery manufacturing has elevated Kocaeli's electricity consumption far above the national average.

The continuous and uninterrupted energy requirements of industrial facilities place Kocaeli in a critical position within national energy supply planning. Organized industrial zones, port facilities, the petrochemical complex, dense commercial activities, and extensive production lines all contribute to a high and dynamic energy demand. For this reason, Kocaeli requires special consideration not only for its current consumption levels but also for the future increase in demand

that is projected to accompany further industrial and infrastructural development (Oskay, 2014).

Another key factor shaping Kocaeli's energy profile is its exceptionally high population density, which ranks among the highest in Türkiye. Although the province has a relatively limited surface area, its strong industrial and service-sector pull has made it a major destination for migration. This leads to rising electricity consumption in both residential and commercial sectors. The high population density intensifies daily fluctuations in energy demand and places additional pressure on the province's energy infrastructure.

Kocaeli's geographical and meteorological characteristics also offer specific advantages for wind energy potential. The coastal districts bordering the Marmara Sea, the topography extending along the gulf, the presence of elevated plateaus, and the wind corridors in the inland regions create favorable conditions for the installation of wind turbines. According to analyses from the REPA, the province exhibits medium-to-high wind speeds particularly along the coastline and in areas where north–south elevation transitions are prominent. This provides an opportunity to utilize local and clean energy sources in a region where industrial activity and thus energy demand is intensely concentrated.

Rapid urbanization, the expansion of industrial activities, and the growing infrastructure supporting electric transportation indicate that energy demand in Kocaeli will continue to rise in the coming years.

In this context, the utilization of domestic, renewable, and low-carbon energy resources is not only an environmental necessity for the province but also a strategic requirement for economic sustainability and energy independence.

Wind energy has the potential to serve as an important complementary resource in meeting Kocaeli's substantial energy needs. The suitability of certain geographical areas within the province allows wind energy generation to be integrated with industrial zones located nearby. This proximity offers advantages such as reduced transmission costs, lower energy losses, and a more balanced regional relationship between production and consumption.

For all these reasons, Kocaeli stands out not only as an economic center of Türkiye but also as a region where strategic decisions in renewable energy planning must be carefully evaluated. Effective wind energy planning can ease the province's overall energy burden and contribute to the formation of a new and sustainable energy structure that supports the national energy transition. For this reason, Kocaeli was selected as the application area for the methodology developed in this study.

2. DETERMINING WIND FARM SUITABILITY AREAS USING GIS

In this chapter, a GIS based analysis was conducted to identify potential areas suitable for wind power plant (WPP) installation in Kocaeli. The suitability zones obtained from the analysis will directly

serve as inputs to the mathematical model developed within this study. First, a literature review on GIS based wind farm site selection is presented; then, the criteria considered in the analysis and the GIS software used are introduced, followed by the findings of the suitability assessment.

2.1. Related Works

The site selection process for wind energy systems is a multi-criteria decision-making (MCDM) problem that requires the simultaneous evaluation of technical, environmental, economic, and social parameters. In the literature, MCDM methods are frequently integrated with GIS to support this complex decision-making process. While GIS allows spatial data to be processed in layered form, MCDM methods such as AHP, VIKOR, PROMETHEE, MARCOS (Measurement of Alternatives and Ranking according to Compromise Solution), and BWM (Best–Worst Method), as well as their fuzzy extensions, are commonly used for criteria weighting and ranking alternatives.

Table 1 summarizes GIS-based wind farm siting studies, including their application areas and the criteria evaluated.

Table 1: Summary of the Literature

Author (Year)	Software	Study Area	Criteria
Özşahin & Kaymaz (2013)	ArcGIS / ArcMap 10	Türkiye – Hatay	Wind speed distribution, power density, capacity factor, roughness, distance to transmission lines, distance to substations, lithology, distance to fault lines, landforms, elevation, slope, aspect, distance to streams, land use, distance to roads
Uzar & Şener (2019)	LiDAR, ArcGIS, eCognition	Türkiye – Kırklareli (Evrencik)	Wind speed, slope, building coverage, vegetation
Moradi et al. (2020)	ArcGIS	Iran – Alborz Province	Wind speed, slope, distance to transmission lines, distance to substations, distance to urban areas, distance to highways and roads
Elmahmoudi et al. (2020)	QGIS 2.18.3	Morocco	Wind speed, slope, land cover/use, distance to settlements, distance to transmission lines, distance to roads
Arca & Keskin Çıtıroğlu (2020)	ArcGIS	Türkiye – Karabük (Yenice)	Wind speed, elevation, slope, aspect, distance to roads, distance to streams, distance to fault lines, lithology, land use, distance to substations
Karipoğlu et al. (2021)	ArcGIS	Türkiye – Kayseri (Develi)	Wind speed, forest areas, military zones, civil and military aviation zones, urbanized areas, special protection zones, agricultural areas, water resources, roads, fault lines, bird migration routes, transmission lines
Hoang et al. (2022)	QGIS	Vietnam – Bac Lieu	Wind speed, elevation, distance to transmission lines, distance to road network, distance to settlements, distance to cultural areas, distance to bird and bat habitats, distance to communication stations
Shorabeh et al. (2022)	QGIS	Iran	Wind speed, elevation, slope, distance to city center, temperature, distance to roads and railways, distance to water resources, distance to protected areas, vegetation density, distance to fault lines
Yousefi et al. (2022)	ArcGIS	Iran – Semnan	Wind speed, slope, distance to transmission lines, distance to substations, distance to urban areas, distance to highways and roads

Author (Year)	Software	Study Area	Criteria
Ekiz et al. (2022)	ArcGIS 10.8	Türkiye – Kocaeli	Wind speed, distance to protected areas, distance to bird migration routes, distance to substations, distance to transmission lines, distance to settlements, distance to highways, distance to fault lines, elevation, slope, distance to rivers, distance to lakes, distance to airports
Huang et al. (2023)	ArcGIS Pro 2.9.2	China – Fujian	Wind speed, slope, distance to grid, distance to roads, distance to urban areas, distance to protected areas, distance to bird areas, land cover/use, soil erosion
Benti et al. (2023)	ArcGIS 10.5	Ethiopia – Wolaita	Wind speed, distance to settlements, distance to transmission lines, distance to rivers, distance to transport network, slope, land cover/use
Yildiz (2024)	ArcGIS	Türkiye – Balıkesir	Wind speed, slope, land cover, distance to transmission lines, distance to substations, distance to road network, distance to settlements, distance to fault lines, distance to ports
Demir et al. (2024)	ArcGIS 10.8	Türkiye – Sivas	Wind speed, wind power density, slope, elevation, aspect, distance to transmission lines, distance to substations, land use, rainfall, distance to road network, population density, distance to settlements, distance to railway, distance to surface water resources, distance to airport, distance to disaster center, distance to tourism center, distance to protected areas, distance to bird habitat
Yousefi et al. (2024)	ArcGIS	Iran – Kermanshah	Wind speed, slope, elevation, distance to transmission lines, distance to substations, distance to road network, land use, distance to settlements, distance to airport, distance to railway, distance to fault line, distance to water sources, distance to protected areas
Placide & Lollchund (2024)	ArcGIS	Burundi	Wind speed, slope, elevation, aspect, distance to transmission lines, distance to road network, land use/land cover, distance to airports, distance to protected areas
Can et al. (2024)	ArcGIS	Türkiye – Çanakkale	Capacity factor, slope, distance to transmission lines, distance to road network, distance to fault lines, distance to settlements
Yaman (2024)	ArcGIS 10.0	Türkiye – Adana	Wind speed, slope, elevation, rock structure, land capability, distance to transmission lines, distance to grid, distance to road network, distance to settlements, distance to bird migration routes, distance to airport, distance to protected areas, distance to water resources, distance to fault lines

Author (Year)	Software	Study Area	Criteria
Şahin et al. (2025)	ArcGIS 10.8	Türkiye – Erzurum	Wind speed, slope, elevation, aspect, land use, distance to transmission lines, distance to substations, distance to settlements, distance to road network, distance to water resources, air temperature, humidity, pressure, surface temperature, solar radiation, distance to fault line, erosion, land capability

2.2. Determination of Criteria for Wind Farm Site Selection

After examining the criteria commonly used in the literature, a set of criteria covering technical, infrastructural, environmental, and social dimensions was established for wind farm site selection within the scope of this book. The selection of criteria was based on their frequency of use in academic studies and the availability of corresponding data. This section briefly explains the role of each selected criterion in the decision-making process.

Elevation: Higher-altitude areas generally experience stronger and more stable wind flows, which can enhance the energy production potential of wind turbines.

Average wind speed: Higher average wind speeds translate into greater energy output, as the efficiency of wind turbines is directly dependent on wind velocity.

Wind capacity factor: Represents the ratio of a wind farm's actual energy production to its theoretical maximum production. A higher capacity factor indicates a more efficient and stable energy generation process.

Wind power density: Refers to the amount of kinetic energy available in the wind. High wind power density values indicate stronger energy production potential.

Distance to water resources and waterways: Locating turbines too close to water bodies may create challenges such as flood risk or regulatory constraints, limiting feasible turbine placement.

Distance to fault lines: Being distant from active faults helps minimize seismic risks and enhances the structural safety of wind farm installations.

Distance to transmission lines: Proximity to transmission lines reduces electricity transportation costs and minimizes energy losses, contributing to more cost-effective operations.

Distance to substations: Being close to substations (power sources/transformers) increases efficiency in electricity transfer from the wind farm to the grid.

Distance to roads: Proximity to transportation networks facilitates construction, operation, maintenance, and logistical processes associated with wind energy projects.

Distance to protected areas: Protected areas were defined to include settlements, agricultural lands, military zones, and natural conservation sites. Maintaining adequate distance from settlements helps prevent potential negative effects on public health and quality of

life, such as noise, visual impact, and shadow flicker. Furthermore, the rotating blades of wind turbines may pose risks to nearby communities. Locating turbines close to residential zones can also reduce social acceptance of the project. Therefore, maintaining sufficient distance from settlements and protected areas is crucial for the sustainability of wind farms and ensuring social compatibility (Ekiz et al., 2022).

2.3. QGIS: An Open-Source GIS Software

QGIS (Quantum Geographic Information System) is an open-source GIS software developed for the visualization, editing, analysis, and mapping of geographic data. Initially created by Gary Sherman in 2002, QGIS joined the Open-Source Geospatial Foundation (OSGeo) in 2007, and its first stable release (version 1.0) was published in 2009. In addition to supporting both raster and vector data formats, QGIS is capable of integrating with various other open-source GIS platforms. Its functionality can be expanded through plugins developed in Python and C++, offering users the ability to tailor the software to specific analytical needs.

Thanks to its user-friendly interface and extensive plugin ecosystem, QGIS enables users to perform complex spatial analyses and produce customized maps efficiently. One of its most significant advantages is that it is completely free and open source. Open-source software allows users to examine, modify, and adapt the source code according to their needs, offering reproducible and distributable solutions for the

broader community. For this reason, QGIS has become widely used in academic and professional environments worldwide, particularly in fields such as environmental sciences, urban planning, energy planning, and disaster management.

QGIS provides a wide range of GIS functions—including mapping, buffering, reclassification, overlay operations, and suitability analyses—which makes it highly suitable for decision-making problems such as site selection. Its scientific use has increased significantly in recent years, a trend also reflected in the academic literature. In a bibliometric analysis conducted by Rosas-Chavoya et al. (2022), the rise in scientific publications focusing on QGIS was found to be parallel to the growing number of code contributors, quantitatively demonstrating the software's expanding impact in academia.

2.4. Processing of Spatial Data

2.4.1. Reclassification Method

In this section, the data sources of the spatial criteria used for wind farm site selection and the suitability ranges defined for each criterion are detailed. The suitability levels assigned to each criterion were converted into a scoring system within the QGIS environment and classified on a scale from 0 to 5. This classification forms the basis of the multi-criteria overlay analysis used in the spatial decision-making process.

The spatial datasets used for wind farm site selection were obtained in two primary formats: raster and vector. Variables with continuous spatial distribution such as elevation, wind speed, wind capacity factor, and wind power density were collected in raster format. Raster datasets consist of a grid structure in which each pixel represents a specific value at a specific location. Such data are typically derived from remote sensing or model outputs and are widely used in mapping surface-related variables (e.g., elevation, temperature, velocity).

In contrast, objects with clearly defined boundaries and locations such as substations, transmission lines, highways, water resources, protected areas, fault lines, and settlement areas were used in vector format. Vector datasets consist of points, lines, and polygons, making them particularly suitable for representing infrastructure, land-use categories, and administrative units.

Before conducting the analysis, all datasets were transformed into the Turkish National Coordinate System (EPSG:5254), and geometric errors were corrected. Then, all vector layers were converted to raster format to ensure uniform spatial resolution across all datasets.

After converting the datasets into raster format, proximity analyses were performed. This type of analysis calculates the distance from each pixel to a given spatial feature, generating a continuous distance surface. For example, when a proximity analysis is applied to a road layer, the distance from every location on the map to the nearest road

is computed. Table 2 presents the data sources and the suitability classification scores used in the analysis.

Table 2: Data Sources and Suitability Classification

Criterion	Criterion Range	Data Source	Score
Elevation (m)	750–1500 450–750 300–450 150–300 0–150 >1500	URL-1	Highly Suitable (5) Very Suitable (4) Suitable (3) Moderately Suitable (2) Low Suitability (1) Not Suitable (0)
Wind speed (m/s)	>6.40 6.05–6.40 5.70–6.05 5.35–5.70 5.00–5.35 0–5.00	Global Wind Atlas (2024)	Highly Suitable (5) Very Suitable (4) Suitable (3) Moderately Suitable (2) Low Suitability (1) Not Suitable (0)
Wind capacity factor	2.1512–9.1329 Divided into 6 equal intervals.	Global Wind Atlas (2024)	Highly Suitable (5) Very Suitable (4) Suitable (3) Moderately Suitable (2) Low Suitability (1) Not Suitable (0)
Wind power density	22.33–1047 Divided into 6 equal intervals.	Global Wind Atlas (2024)	Highly Suitable (5) Very Suitable (4) Suitable (3) Moderately Suitable (2) Low Suitability (1) Not Suitable (0)
Distance to water resources (m)	>15000 12000–15000 9000–12000 6000–9000 3000–6000 <3000	URL-2	Highly Suitable (5) Very Suitable (4) Suitable (3) Moderately Suitable (2) Low Suitability (1) Not Suitable (0)
Distance to fault lines (m)	>5000 4000–5000 3000–4000 2000–3000 1000–2000 <1000	URL-2	Highly Suitable (5) Very Suitable (4) Suitable (3) Moderately Suitable (2) Low Suitability (1) Not Suitable (0)
Distance to transmission lines (m)	100–500 500–1000 1000–2500 2500–5000 5000–10000 <100 or >10000	URL-2	Highly Suitable (5) Very Suitable (4) Suitable (3) Moderately Suitable (2) Low Suitability (1) Not Suitable (0)

Criterion	Criterion Range	Data Source	Score
Distance to substations (m)	<1000	URL-2	Highly Suitable (5)
	1000–5000		Very Suitable (4)
	5000–10000		Suitable (3)
	10000–15000		Moderately Suitable (2)
	15000–25000		Low Suitability (1)
	>25000		Not Suitable (0)
Distance to roads (m)	100–1000	URL-2	Highly Suitable (5)
	1000–2000		Very Suitable (4)
	2000–3000		Suitable (3)
	3000–4000		Moderately Suitable (2)
	4000–10000		Low Suitability (1)
	<100 or >10000		Not Suitable (0)
Distance to protected areas (m)	>4000	URL-2	Highly Suitable (5)
	3500–4000		Very Suitable (4)
	3000–3500		Suitable (3)
	2500–3000		Moderately Suitable (2)
	2000–2500		Low Suitability (1)
	0–2000		Not Suitable (0)

In determining the classification scores, the study by Ekiz et al. (2022) was taken as a reference. However, since the variables of wind capacity factor and wind power density were classified by directly dividing their value ranges into six equal intervals, no external reference was used for these two variables.

After the completion of the distance analyses, a reclassification procedure was applied. Reclassification is the process of converting a continuous variable into categorical suitability classes based on predefined threshold values. In this study, all criteria were divided into six suitability levels, ranging from “Highly Suitable (5)” to “Not Suitable (0),” as specified in Table 2. This transformation enabled criteria measured on different scales to be made comparable and suitable for multi-criteria evaluation. Raster datasets obtained directly in raster format were reclassified according to the 0–5 scoring scale and subsequently visualized. Within this scope, the reclassified maps

of elevation, wind speed, wind capacity factor, and wind power density for Kocaeli are presented in Figure 2.

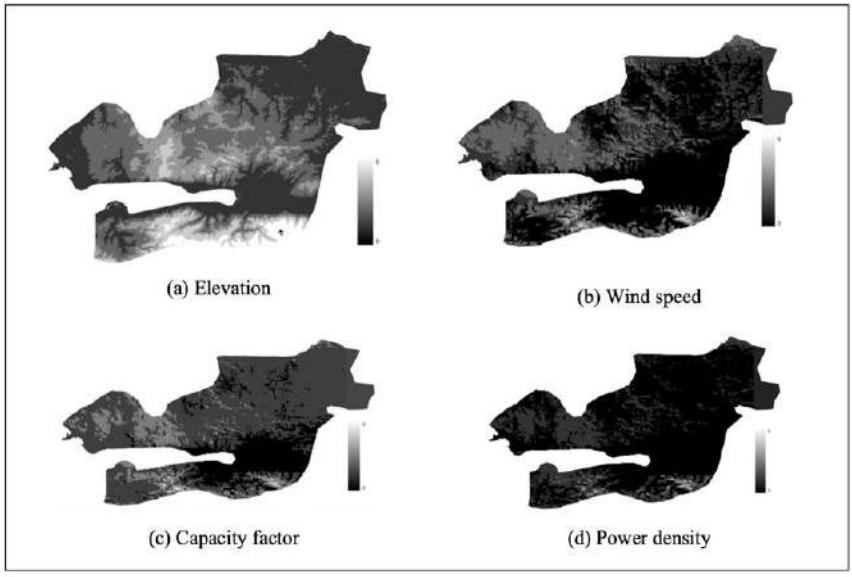

Figure 2: Reclassified maps of Kocaeli Province: (a) elevation, (b) wind speed, (c) capacity factor, and (d) power density.

The vector datasets water resources, fault lines, transmission lines, substations, roads, and protected areas are presented together on a single map in Figure 3.

All vector datasets presented collectively in Figure 3 were converted into raster format and reclassified according to the defined suitability intervals. The steps of this procedure are illustrated using the "transmission line" dataset as an example.

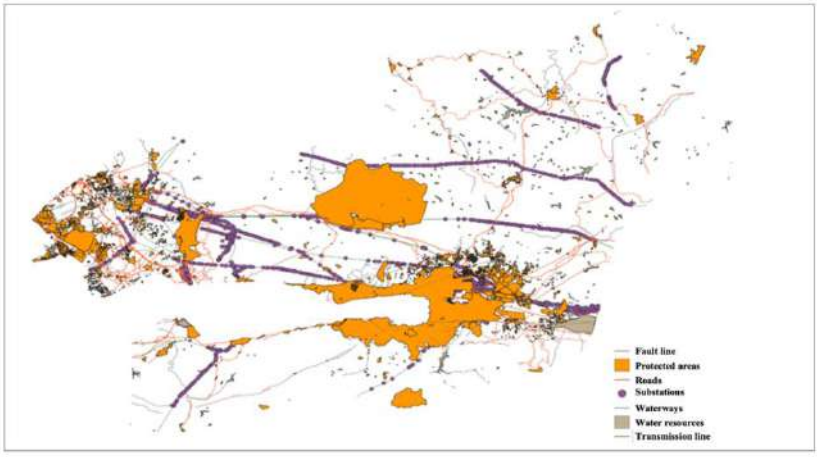

Figure 3: Vector datasets for Kocaeli

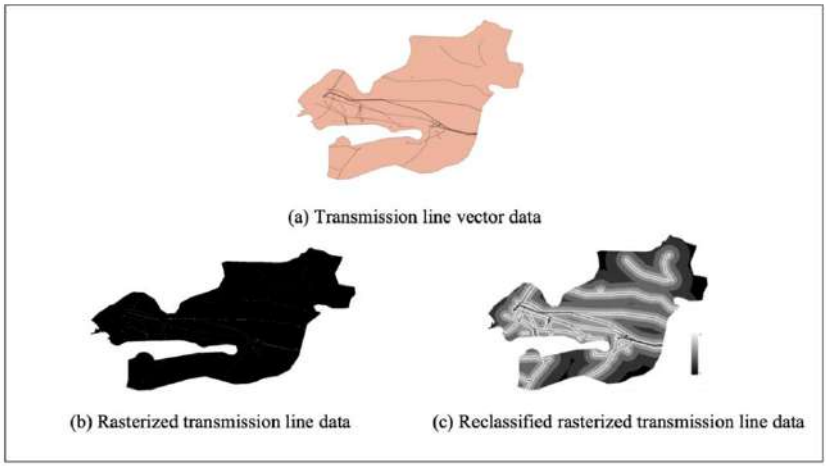

Figure 4: Rasterization and reclassification of the "transmission line" vector data for Kocaeli

Figure 4 presents (a) the vector dataset of transmission lines for Kocaeli, (b) its raster-converted form, and (c) its final reclassified output.

2.4.2. Overlay Analysis

Overlay analysis is a method used in spatial decision-making processes whereby different thematic layers are superimposed, allowing each location to be evaluated with an integrated suitability score. As a result of the reclassification procedure applied in this study, each raster layer was assigned suitability scores ranging from 0 to 5. Subsequently, assuming equal importance for all criteria, the suitability score for each pixel was calculated by summing the scores of all criteria corresponding to that location.

The suitability scores obtained from the overlay analysis for Kocaeli will serve as the initial input data for the linear programming model presented in the following section. As a result of the analysis, the total suitability scores for each cell were calculated to range between 0 and 25.5. The spatial suitability map generated based on these values is presented in Figure 5.

Since the highest suitability score for wind turbine installation was calculated as 25.5, regions with suitability scores greater than 20, 21, 22, 23, and 24 were individually analyzed in QGIS to allow for a more detailed examination of the results. The spatial distributions corresponding to each threshold value are visualized in Figure 6.

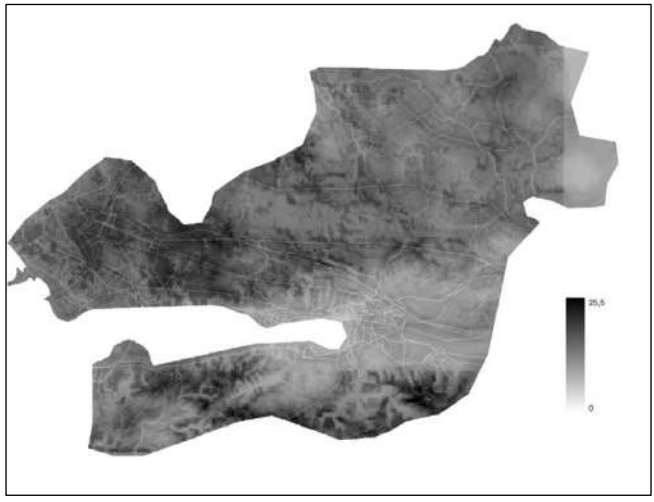

Figure 5: Overlay analysis for Kocaeli

This analysis provides a comparative overview of regions with varying suitability levels and offers visual support prior to model development. Based on the findings, the mathematical model was designed to include only the areas with wind energy suitability scores of 23 and above. The selection of this threshold was based on prioritizing areas with high energy generation potential, while also ensuring that the model does not include too few or excessively many regions—both of which would hinder meaningful generalization or reduce the model's applicability. Thus, the chosen threshold aims to balance the inclusion of a sufficient number of alternatives while keeping the decision space at a rational and manageable level.

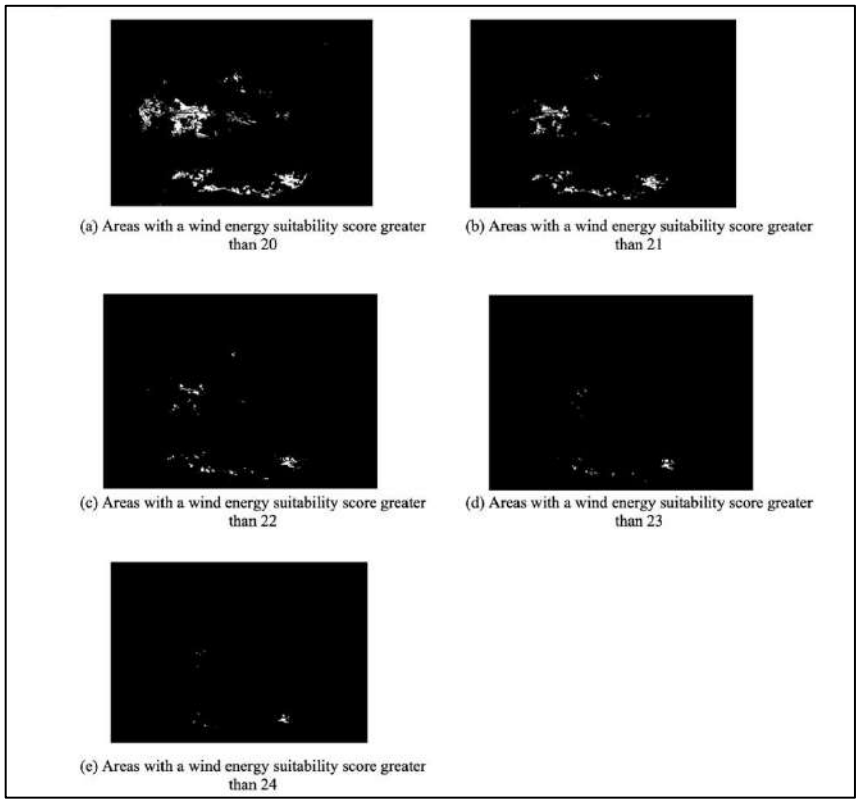

Figure 6: Spatial distributions of wind energy suitability scores for Kocaeli

2.4.3. Polygonization of Suitable Areas

Wind energy suitability areas with scores of 23 and above were analyzed in detail to form the basis of the site selection problem. Using QGIS, the suitability map obtained in raster format was converted into vector format (polygonized), and each suitable area was digitized as an independent polygon, as illustrated in Figure 7. This conversion enables various calculations to be performed for the high-suitability areas.

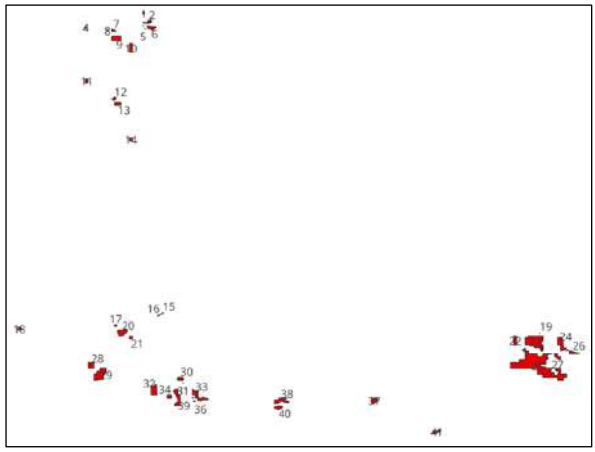

Figure 7: Polygonization of areas with suitability scores greater than 23

The representation of the suitable areas on the map of Kocaeli is provided in Figure 8, while their visualization on Google Maps is presented in Figure 9.

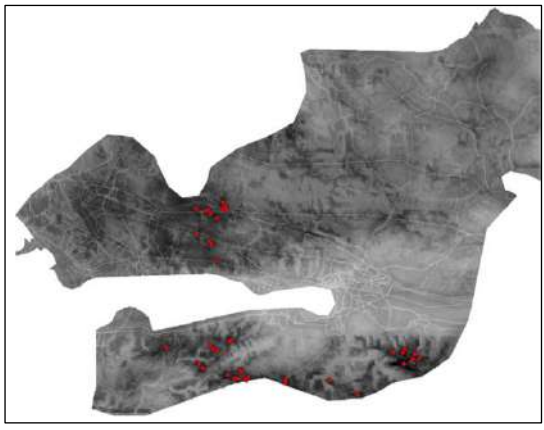

Figure 8: Display of areas with wind energy suitability scores greater than 23 on the map of Kocaeli

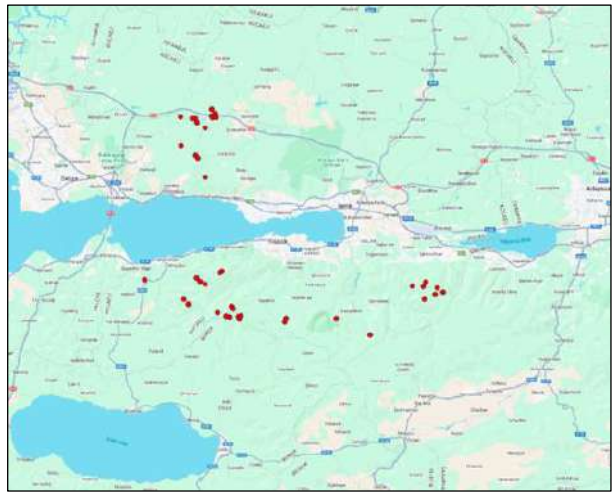

Figure 9: Visualization of areas with wind energy suitability scores greater than 23 on Google Maps

Following the polygonization process, the area of each polygon was calculated in QGIS, and the centroid coordinates of each region were determined. These points were used both as reference locations in spatial analyses and as fixed representative points for each region in the mathematical modeling process. As an example, the centroid points of seven selected regions are presented in Figure 10.

The identified centroid points were used to calculate the distances between the corresponding regions and the nearest substations. The map used for this calculation is shown in Figure 11.

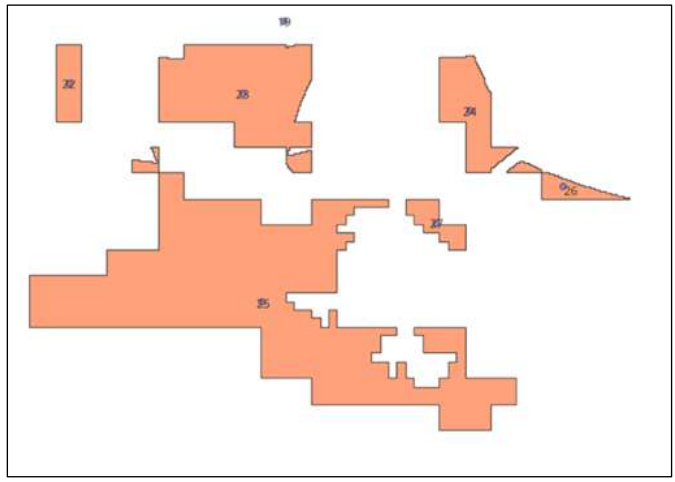

Figure 10: Determination of centroid points for polygons (illustrative example)

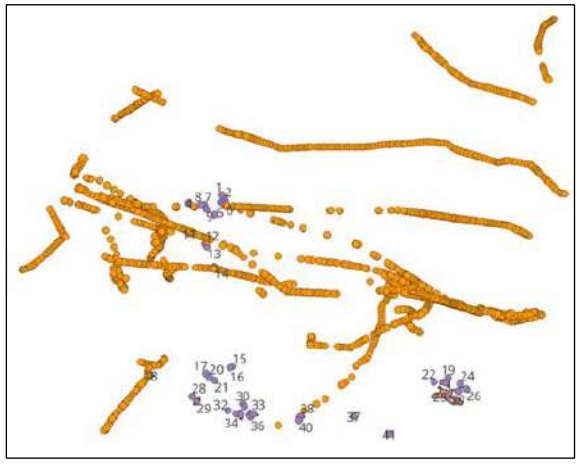

Figure 11: Calculation of the distance from centroids to the nearest substation

To clearly define the dimensional characteristics of the suitable areas such as their width and length the suitability regions were converted into rectangular forms, thus providing standardized geometric measurements for each area. This transformation established a

framework that facilitates the structured representation of site locations in the modeling process and simplifies the application of spatial constraints.

Table 3 presents the width and length values of the rectangularized regions suitable for wind turbine installation, along with the distance from each area's centroid to the nearest substation and the spatial coordinates (X and Y) of these centroids. The X and Y coordinates used here are metric coordinates based on a projection system suitable for processing within the QGIS environment, rather than geographic latitude–longitude values.

Table 3: Parameters of Potential Wind Turbine Installation Areas

No	Width (m)	Length (m)	Distance to Nearest Substation (m)	Centroid X Coordinate	Centroid Y Coordinate
1	208.8769	136.0688	1,706.1990	727305	4531061
2	626.5699	284.0419	860.1540	727778	4530355
3	116.5497	16.2680	892.9230	727299	4530009
4	55.6385	16.2680	783.1780	722535	4529716
5	41.6406	40.9307	597.3830	727498	4529788
6	643.6462	298.2864	311.6120	727992	4529853
7	327.4551	194.1772	1,431.8560	724853	4529531
8	53.7275	91.8179	960.9590	724345	4529522
9	692.8479	357.4789	1,674.3460	725123	4528898
10	240.0852	630.6937	2,083.8300	726357	4528145
11	226.3838	324.6933	291.3460	722788	4525294
12	307.1592	238.8960	434.1670	725111	4523881
13	431.8607	216.7012	748.5690	725422	4523467
14	226.2315	209.0261	283.4090	726617	4520580

No	Width (m)	Length (m)	Distance to Nearest Substation (m)	Centroid X Coordinate	Centroid Y Coordinate
15	229.3928	134.2726	9,874.2520	725885	4505093
16	178.5861	89.7069	9,799.0960	717894	4504580
17	144.0096	76.4795	6,457.0370	761073	4505660
18	212.0438	212.0438	469.3270	726416	4504547
19	39.8396	39.8396	7,747.5320	727178	4504161
20	693.2720	440.8946	7,242.5110	759046	4505001
21	224.6763	211.0130	8,030.6240	760700	4504959
22	226.9499	630.7963	7,436.4120	762870	4504870
23	1,272.8044	1,035.0965	8,138.9840	762590	4503796
24	664.5976	943.1546	9,410.6810	723966	4501732
25	3,991.8780	2,194.5789	9,995.9380	724714	4500994
26	1,005.4241	283.4569	10,553.8610	731396	4500882
27	499.9861	381.4909	10,183.2520	731630	4500547
28	423.7410	408.9506	7,022.0370	729248	4499862
29	826.7496	828.0991	8,005.6400	730536	4499390
30	415.9470	205.0346	6,070.2030	732463	4499356
31	38.6591	39.0809	5,681.9410	732599	4499054
32	429.3455	696.8612	7,615.3460	747524	4499628
33	1,183.7600	767.4738	4,066.6240	739785	4499344
34	313.8813	213.3432	6,292.1900	731210	4499289
35	91.8494	60.7991	4,420.4570	739617	4498770
36	29.6515	64.0724	4,247.2260	752797	4497230
37	416.1798	413.8837	7,272.9000	729697	4506236
38	1,054.4328	430.2926	1,026.2280	729372	4506066
39	558.2912	1,133.1462	5,651.7650	760956	4502991
40	587.3167	256.8356	1,676.6530	763782	4504182
41	589.8062	270.7690	10,051.3330	732914	4499522

In conclusion, the spatial analyses conducted in this chapter identified the areas suitable for wind turbine installation and systematically presented the physical and spatial parameters associated with these regions. The data obtained from these analyses will serve as the fundamental inputs for the mathematical model to be developed in the next stage.

3. WIND TURBINE SITING FOR KOCAELI USING A MIXED-INTEGER LINEAR PROGRAMMING MODEL

In this chapter, a mixed-integer linear programming model is developed to determine the optimal placement of onshore wind turbines within the suitable areas identified for Kocaeli using GIS analyses. The proposed approach is generalizable to other provinces with similar geographical and infrastructural characteristics and provides a methodological framework that can support regional wind energy planning efforts.

3.1. Wind Turbines and Their Costs

Wind turbines are systems designed to convert wind energy into electrical energy and consist of several complementary technical components. The first of these is the rotor. The rotor, composed of blades and the central hub structure to which the blades are attached, captures wind energy and converts it into rotational motion. This rotational motion constitutes the first step of the mechanism that enables the turbine to generate electricity.

Located at the top of the turbine and directly connected to the rotor, the nacelle is the most complex electrical and mechanical unit of the system. It houses all the equipment required to convert the rotor's rotational motion into electrical energy. The tower elevates the rotor and the nacelle to a specific height above the ground, allowing the turbine to benefit from stronger and more consistent wind flows at higher altitudes. Finally, the foundation ensures that the entire turbine system is firmly anchored to the ground. It plays a critical role in maintaining structural integrity and keeping the turbine stable against external loads.

Wind turbine manufacturers develop various designs tailored to different site conditions, grid connection requirements, and policy frameworks. Turbines with larger rotor diameters can produce more energy under the same wind speed conditions. High-capacity turbines increase the feasibility of large-scale projects and reduce the total installation cost per megawatt by lowering certain cost components.

Between 2000 and 2002, wind turbine prices experienced a decline; however, after this period, sharp price increases were observed due to rising commodity prices—particularly cement, copper, iron, and steel—and supply chain bottlenecks. This trend coincided with a period during which governments intensified policy support for wind energy investments. As a result, the imbalance between high demand and limited supply enabled turbine manufacturers to achieve substantial profit margins.

As supply chains expanded and manufacturing capacities increased, wind turbine prices peaked in many markets between 2007 and 2010, after which they entered a downward trend. By the end of 2019, turbine prices had decreased by approximately 44% to 78%. The intensifying competition among manufacturers exerted downward pressure on profit margins, creating cost advantages for consumers. Competitive renewable energy auctions implemented by many countries further reinforced this process. Moreover, the price gap between turbines with different rotor diameters has narrowed. According to 2019 data, turbines with rotor diameters exceeding 100 meters had an average price of 785 USD/kW, whereas those with rotor diameters below 100 meters averaged 752 USD/kW.

According to the IRENA (2020) Renewable Energy Cost Database, the average total installation cost of onshore wind projects decreased from 1,949 USD/kW in 2010 to 1,473 USD/kW in 2019.

Figure 12 illustrates the changes in total installation costs for 15 countries that have significant relevance to global wind energy markets and sufficient time-series data. While some countries have achieved substantial cost reductions, the decline in Türkiye remained at approximately 2%. However, when making such comparisons, it should be noted that the starting year of the available data differs across countries. In more competitive markets, more pronounced decreases in total installation costs have been observed over longer time periods.

Nevertheless, variations between countries are natural due to differences in local conditions. Factors such as constraints related to transportation logistics, domestic manufacturing policies, land-use regulations, and labor costs are among the primary drivers of these differences. For Türkiye, installation costs in 2019 generally ranged between 1,700 USD/kW and 1,900 USD/kW.

The capacity factor is calculated by dividing the actual energy produced by a wind plant over a given period (typically one year) by its theoretical maximum production over the same period. It mainly depends on two variables: the quality of the wind resource at the installation site, and the technical characteristics of the turbine and auxiliary systems. Over the past decade, many markets have shifted toward advanced and efficient turbine technologies with larger rotor diameters and higher tower heights. This trend has significantly increased energy output and capacity factors. Indeed, while the average capacity factor for onshore wind energy projects was around 27% in 2010, it had risen to approximately 36% by 2019.

Operation and maintenance (O&M) costs are among the key components determining the levelized cost of energy (LCOE) for onshore wind and can account for up to 30% of the total LCOE. However, technological innovations, increased competition among service providers, and accumulated operational experience have contributed to a reduction in these costs. According to data presented by IRENA, O&M costs for onshore wind energy between 2016 and

2018 ranged from 33 USD/kW annually in Denmark to 56 USD/kW in Germany (IRENA, 2020).

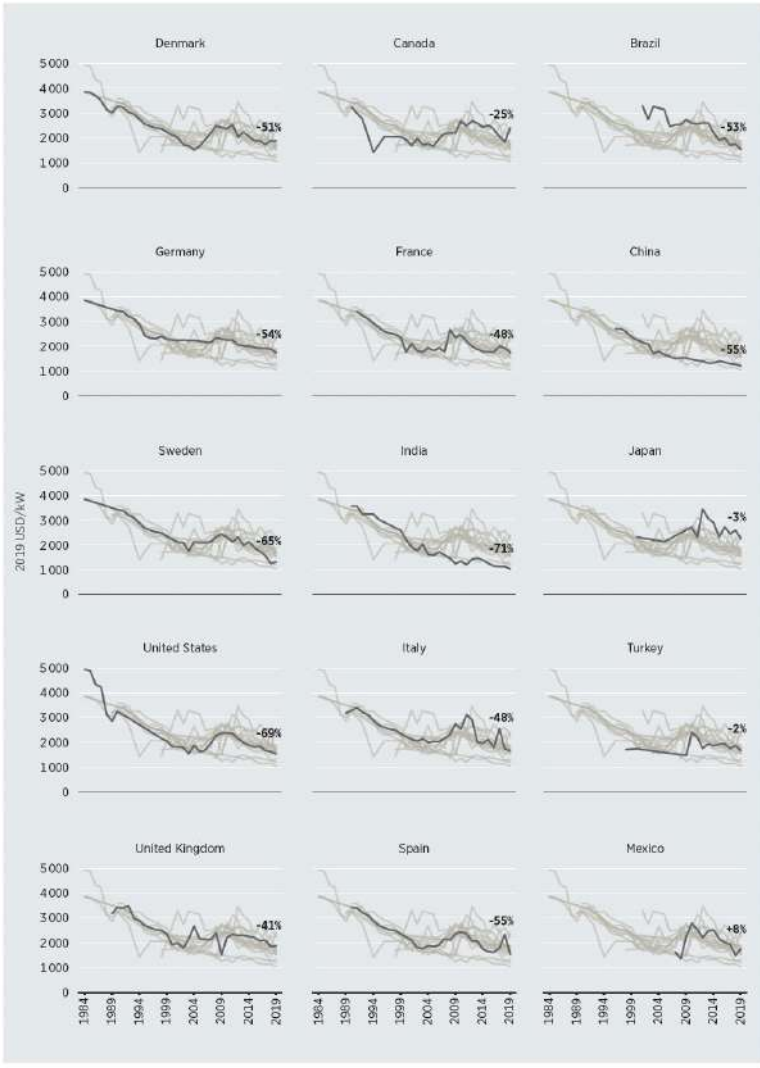

Figure 12: Average total installation costs for onshore wind energy in 15 countries (1984–2019)

Reference: IRENA, 2020.

3.2. Mathematical Model Formulation

In this section, the objective is to place different types of wind turbines in the candidate areas identified through GIS in a manner that minimizes the total cost.

3.2.1. Selection of Turbine Types

The onshore wind turbine types used in this study were selected from among the models that are commonly preferred in real-world project applications.

Table 4: Parameters by Turbine Type

Turbine Type	Model Name	Power (MW)	Rotor Diameter (m)	Annual Generation (GWh)	Tower Height (m)	Nacelle Length (m)	Nacelle Width (m)	Nacelle Height (m)	Noise Level (dB)	Carbon Footprint (gCO_2e/kWh)
t1	RPWM	2.00	75	5500	70	10.40	3.50	4.00	103.0	7.1
t2	VST1	2.00	90	7000	80	10.40	3.50	4.00	104.0	7.2
t3	VST2	2.00	110	9000	95	10.40	3.50	4.00	107.6	7.2
t4	VST3	2.00	100	8100	125	10.40	3.50	4.00	105.0	7.2
t5	VST4	2.10	116	9800	124	10.40	3.50	4.00	109.5	7.2
t6	VST5	2.20	120	10200	137	10.40	3.50	4.00	110.5	6.8
t7	VST6	3.45	117	14000	116	12.80	4.20	3.40	106.8	5.1
t8	VST7	4.20	117	14000	91	12.80	4.20	3.40	106.0	4.4
t9	VST8	3.45	126	14000	166	12.80	4.20	3.40	105.8	6.4
t10	VST9	3.45	136	15000	166	12.80	4.20	3.40	105.5	7.6
t11	VST10	4.20	136	15100	166	12.96	3.98	3.50	103.9	5.6
t12	VST11	4.50	136	15000	112	12.96	3.98	3.50	103.9	4.9
t13	VST12	4.20	150	17500	166	12.96	3.98	3.50	104.9	7.3
t14	VST13	4.50	150	16000	105	12.96	3.98	3.50	107.6	5.6
t15	VST14	4.50	163	22000	126	12.96	3.98	3.50	107.4	4.7
t16	VST15	6.00	150	21000	169	12.96	3.98	3.50	104.9	5.6
t17	VST16	6.20	162	22500	169	12.96	3.98	3.50	104.8	6.2
t18	VST17	7.20	162	25500	169	12.96	3.98	3.50	105.5	7.1
t19	VST18	7.20	172	27000	199	12.96	3.98	3.50	107.8	6.9

In the process of selecting turbine types, product catalogs of wind turbine manufacturers that are widely recognized in Türkiye and around the world were examined in detail. Since the catalogs of a commonly used manufacturer provide comprehensive technical specifications for each model, 18 turbine types were selected from the most recent versions of these catalogs. As all models offered by this manufacturer consist of large-scale turbines with rotor diameters of 90 meters and above, an additional turbine with a rotor diameter of 75 meters—commonly used in medium-scale projects—was incorporated into the model from the catalog of another manufacturer. Catalogs belonging to other producers did not include all the technical and economic parameters required for this study; therefore, only turbines from these two manufacturers were considered. The turbine types used in this research and their associated technical and environmental parameters are presented in Table 4 (Vestas, 2025a; 2025b; 2025c).

3.2.2. Calculation of the Capacity Factor

The capacity factor represents the ratio between the actual annual energy production of a wind turbine and the theoretical maximum energy it could generate if it operated at full capacity throughout the entire year. In this study, the capacity factor values were calculated based on the annual energy production figures provided in the manufacturers' catalogs, which correspond to a constant wind speed of 7.5 m/s.

The capacity factor was calculated using Equation (1) and the resulting values are presented in Table 5.

$$\text{Capacity Factor} = \frac{\text{Actual Annual Production (MWh)}}{\text{Power (MW)} \times 8760 \text{ hours/year}} \quad (1)$$

Table 5: Determination of the Capacity Factor

Turbine Type	Model Name	Power (MW)	Annual Production (MWh)	Capacity Factor
t1	RPWM	2.00	5,500	0.3139
t2	VST1	2.00	7,000	0.3995
t3	VST2	2.00	9,000	0.5137
t4	VST3	2.00	8,100	0.4623
t5	VST4	2.10	9,800	0.5327
t6	VST5	2.20	10,200	0.5293
t7	VST6	3.45	14,000	0.4632
t8	VST7	4.20	14,000	0.3805
t9	VST8	3.45	14,000	0.4632
t10	VST9	3.45	15,000	0.4963
t11	VST10	4.20	15,100	0.4104
t12	VST11	4.50	15,000	0.3805
t13	VST12	4.20	17,500	0.4756
t14	VST13	4.50	16,000	0.4059
t15	VST14	4.50	22,000	0.5581
t16	VST15	6.00	21,000	0.3995
t17	VST16	6.20	22,500	0.4143
t18	VST17	7.20	25,500	0.4043
t19	VST18	7.20	27,000	0.4281

3.2.3. Calculation of Costs

According to IRENA's 2019 data, the average unit price of wind turbines with rotor diameters greater than 100 meters was 785 USD/kW, while those with rotor diameters below 100 meters had an average price of 752 USD/kW. Globally, the average total installation cost for onshore wind projects was reported as 1,473 USD/kW. In

Türkiye, installation costs in 2019 generally ranged between 1,700 USD/kW and 1,900 USD/kW. In this study, the average installation cost for Türkiye was taken as 1,800 USD/kW, and two main cost components were considered in the turbine-related cost calculations (IRENA, 2020):

Turbine purchase cost: This cost was calculated by multiplying the turbine's rated power (MW) by the unit turbine price (USD/kW), which varies depending on the rotor diameter.

Turbine installation cost: Based on IRENA data, the Türkiye-specific average installation cost (1,800 USD/kW) was multiplied by the turbine's rated power to obtain the installation cost.

According to data published by IRENA, the annual O&M costs for onshore wind energy projects ranged between 33 USD/kW and 56 USD/kW during the period 2016–2018. In this study, a conservative approach was adopted, and the annual O&M cost for Türkiye was assumed to be 56 USD/kW. The total O&M cost was calculated by multiplying the turbine's installed capacity (MW) by the unit cost. Of the resulting total cost, 70% was allocated to maintenance costs and 30% to operation costs. These cost components are presented in Table 6 according to turbine type.

Table 6: Calculation of Installation, Maintenance, and Variable Costs

Turbine Type	Model Name	Power (MW)	Turbine Purchase Cost ($)	Turbine Installation Cost ($)	Total Installation Cost ($)	Maintenance Cost ($)	Variable Cost ($)
t1	RPWM	2.00	1,504,000	3,600,000	5,104,000	78,400	33,600
t2	VST1	2.00	1,504,000	3,600,000	5,104,000	78,400	33,600
t3	VST2	2.00	1,570,000	3,600,000	5,170,000	78,400	33,600
t4	VST3	2.00	1,570,000	3,600,000	5,170,000	78,400	33,600
t5	VST4	2.10	1,648,500	3,780,000	5,428,500	82,320	35,280
t6	VST5	2.20	1,727,000	3,960,000	5,687,000	86,240	36,960
t7	VST6	3.45	2,708,250	6,210,000	8,918,250	135,240	57,960
t8	VST7	4.20	3,297,000	7,560,000	10,857,000	164,640	70,560
t9	VST8	3.45	2,708,250	6,210,000	8,918,250	135,240	57,960
t10	VST9	3.45	2,708,250	6,210,000	8,918,250	135,240	57,960
t11	VST10	4.20	3,297,000	7,560,000	10,857,000	164,640	70,560
t12	VST11	4.50	3,532,500	8,100,000	11,632,500	176,400	75,600
t13	VST12	4.20	3,297,000	7,560,000	10,857,000	164,640	70,560
t14	VST13	4.50	3,532,500	8,100,000	11,632,500	176,400	75,600
t15	VST14	4.50	3,532,500	8,100,000	11,632,500	176,400	75,600
t16	VST15	6.00	4,710,000	10,800,000	15,510,000	235,200	100,800
t17	VST16	6.20	4,867,000	11,160,000	16,027,000	243,040	104,160
t18	VST17	7.20	5,652,000	12,960,000	18,612,000	282,240	120,960
t19	VST18	7.20	5,652,000	12,960,000	18,612,000	282,240	120,960

3.2.4. Estimation of Scrap Value

At the end of their economic lifetime, wind turbines retain a recoverable scrap value based on the recyclable materials contained within their components. This value constitutes an important element of total cost assessments and should therefore be included in economic analyses. In this study, the estimation of scrap value was conducted using references from the literature and several technical assumptions.

In the study by Şentürk and Oğuz (2020), the scrap value of an Enercon E-40 wind turbine was calculated as an illustrative case. In the referenced model, the tower height was taken as 44 meters, the nacelle weight as 19.77 tons, and the tower weight as 29.91 tons. The authors classified the recoverable materials based on turbine components: iron from the nacelle and tower, composite material from the rotor, concrete from the foundation, and aluminum from electronic systems. However, concrete and composite materials were assumed to have no scrap value.

For the purposes of the present study, the height of each turbine tower was proportionally scaled relative to the 44-meter reference tower to estimate the corresponding tower weights. Although the original study did not provide the exact nacelle dimensions, manufacturer catalogues indicate approximate dimensions of 7.25 m × 3.25 m × 3.25 m for the nacelle of the reference model. Accordingly, the nacelle volume of each turbine type was calculated relative to the reference nacelle volume, and proportional scaling was used to estimate nacelle weight.

Şentürk and Oğuz (2020) reported that 845 tons of iron could be recovered from a combined nacelle and tower weight of 49.68 tons. Using this ratio, the amount of recoverable iron scrap for each turbine type in this study was estimated. The same study indicated that 132 tons of aluminum could be recovered from the electronic systems. Due to the lack of detailed information on electronic components, the aluminum scrap quantity for each turbine type was estimated by

applying the ratio of aluminum to iron obtained in the reference study (0.132 / 0.845 ≈ 0.156).

Table 7: Calculation of Scrap Value

Turbine Type	Estimated Tower Weight (t)	Nacelle Volume (m^3)	Estimated Nacelle Weight (t)	Total Weight (t)	Total Iron (t)	Iron Scrap Value ($)	Aluminum (t)	Aluminum Scrap Value ($)	Total Scrap Value ($)
t1	47.58	145.60	37.59	85.17	1,448.70	467,090	226	478,662	945,708
t2	54.38	145.60	37.59	91.97	1,564.32	504,369	244	516,864	1,021,186
t3	64.58	145.60	37.59	102.17	1,737.75	560,287	271	574,168	1,134,402
t4	84.97	145.60	37.59	122.56	2,084.62	672,123	326	688,774	1,360,835
t5	84.29	145.60	37.59	121.88	2,073.06	668,395	324	684,954	1,353,287
t6	93.13	145.60	37.59	130.72	2,223.37	716,857	347	734,617	1,451,408
t7	79.19	182.78	47.19	126.38	2,149.62	693,081	336	710,251	1,403,268
t8	62.20	182.78	47.19	109.39	1,860.57	599,884	291	614,746	1,214,574
t9	112.84	182.78	47.19	160.03	2,721.95	877,610	425	899,353	1,776,881
t10	112.84	182.78	47.19	160.03	2,721.95	877,610	425	899,353	1,776,881
t11	112.84	180.53	46.61	159.45	2,712.06	874,423	424	896,086	1,770,428
t12	76.13	180.53	46.61	122.74	2,087.71	673,118	326	689,794	1,362,850
t13	112.84	180.53	46.61	159.45	2,712.06	874,423	424	896,086	1,770,428
t14	71.38	180.53	46.61	117.98	2,006.77	647,023	313	663,053	1,310,015
t15	85.65	180.53	46.61	132.26	2,249.58	725,308	351	743,277	1,468,518
t16	114.88	180.53	46.61	161.49	2,746.75	885,607	429	907,547	1,793,071
t17	114.88	180.53	46.61	161.49	2,746.75	885,607	429	907,547	1,793,071
t18	114.88	180.53	46.61	161.49	2,746.75	885,607	429	907,547	1,793,071
t19	135.27	180.53	46.61	181.88	3,093.61	997,443	483	1,022,154	2,019,504

The monetary value of scrap materials was determined based on forecasted scrap metal prices for the year 2025. Accordingly, the scrap iron price was taken as 12,500 TRY per ton, which corresponds to approximately 322.39 USD/ton based on the current exchange rate. The scrap aluminum price was accepted as 82,000 TRY per ton, equivalent to 2,115.11 USD/ton. Based on these unit prices, the total scrap value for each turbine type was calculated by multiplying the

estimated amounts of iron and aluminum by their respective unit prices, as presented in Table 7.

In the model, the scrap values expected to be obtained at the end of the turbines' economic lifetime were discounted to their present value. For this purpose, a discount rate of 10% was adopted, and the scrap value calculated for each turbine type was converted into its present monetary equivalent at the end of a 25-year lifetime using Equation (2). Here, *NPV* denotes the net present value, R_t represents the net cash flow at time *t*, *I* is the discount rate, and *t* refers to the time period of the cash flow.

$$\mathrm{NPV} = \frac{R_t}{(1+i)^t} \tag{2}$$

3.2.5. Other Parameters and Assumptions

To ensure that the model produces realistic and applicable solutions, several parameters were defined based on real-world field practices and literature-supported assumptions. The parameters and assumptions used in the model are presented below.

Economic lifetime: Considering the commercial usage period of wind turbines, the economic lifetime was set to 25 years. This value is widely accepted in both the literature and real-world wind farm feasibility studies (Tost et al., 2024; Onat et al., 2016; Yıldırım, 2017).

Total energy target: This represents the total amount of energy the model aims to produce in the first year. The target depends on the

capacity factor and the energy losses that occur during the transmission of electricity from wind turbines to substations. Multiple scenarios were evaluated in this study. Details regarding the total energy target are presented in Section 3.2.11.

Land cost and budget constraint: The unit land cost was assumed as 3 USD/m², and the total budget allocated for land use was limited to 3,000,000 USD (Kabak and Taşkınöz, 2020).

Cost of transmission to substations: The cost of energy transmission from wind turbines to substations was set to 0.003 USD per meter, based on Kabak and Taşkınöz (2020). This parameter covers the costs associated with transmission line installation, operation, and maintenance.

Infrastructure cost: The infrastructure cost was defined as 150,000 USD per turbine and includes construction expenses, site preparation, and connection infrastructure. This cost reflects one-time expenses incurred during the first year, particularly for turbine-specific access roads and substation switchyard connections (Yıldırım, 2017).

Project development and licensing costs: Project development cost was defined as 25,000 USD/MW per turbine, covering feasibility studies, site measurements, permitting processes, environmental impact assessments, and other technical analyses. Licensing cost was similarly defined as 10,000 USD/MW (Yıldırım, 2017). Both costs occur only in the initial year of investment.

Maintenance equipment cost: A maintenance equipment cost of 25,000 USD per turbine was included. This fixed cost covers long-term tools, spare parts, and service support systems required in maintenance operations.

Labor cost: Labor costs associated with installation and maintenance are included under respective cost categories. Additionally, security services were assumed for operational safety, with one security officer assigned per four turbines. Since each region requires independent security coverage, personnel needs were calculated per region. Each security officer's annual salary was set at 12,000 USD (Yıldırım, 2017), repeating annually throughout the 25-year economic lifetime.

Other costs: An additional fixed cost of 10,000 USD per turbine was defined to represent unforeseen technical and operational support expenses throughout the project lifecycle.

Minimum distance between region centers: To reduce wake effects, minimize inter-turbine turbulence, and enhance energy production efficiency, the literature recommends spacing wind turbines approximately 7–9 rotor diameters apart. In practice, this distance may be reduced slightly for large-scale turbines. Some studies indicate that turbines may be placed at a minimum spacing of 3 rotor diameters horizontally and 5 rotor diameters vertically (Duval, 2025).

In this model, the largest turbine has a rotor diameter of 172 m; thus, 5 rotor diameters equal 860 meters. Therefore, a minimum distance of 860 meters between any two installation regions was required. This

ensures that adequate spacing is maintained not only within regions but also between turbines located in different regions, reducing wind interference and improving system safety.

Annual cost escalation rate: Since certain cost components are expected to increase over time, an annual cost escalation rate of 7.5% was applied. This reflects sectoral inflation, labor market wage dynamics, and increasing service costs in the energy sector. The escalation rate applies to recurring costs such as maintenance, variable operating expenses, and security personnel salaries.

The value of a recurring cost In year a, denoted by g_a, is calculated using compounded growth based on its initial value g_1 and annual escalation rate κas expressed in Equation (3).

$$g_a = g_1 \cdot (1 + \kappa)^{a-1} \tag{3}$$

Annual decrease in energy production: Wind turbines experience performance degradation over time, leading to small but continuous reductions in energy output. To reflect this reality, an annual decrease rate of 0.5% was assumed in the model. This loss may arise from aging turbine components, surface contamination or erosion on rotor blades, mechanical wear, and general efficiency declines within the system. Accordingly, this reduction is applied each year in the energy production calculations, ensuring that performance over the economic lifetime of the turbine is represented more realistically. The annual production efficiency factor $\delta(a)$, based on a constant yearly loss rate

λ, is calculated using the compound multiplier presented in Equation (4).

$$\Delta(a) = (1 - \lambda)^{a-1} \quad (4)$$

Minimum regional energy production requirements: As shown in Figure 7, the 41 potential installation sites were grouped into four main geographical regions based on spatial proximity. These main region clusters were defined as follows:

- *Main Region 1:* k1–k14
- *Main Region 2:* k15–k18, k20, k21, k28–k36
- *Main Region 3:* k37–k41
- *Main Region 4:* k19, k22–k27

In the model, a minimum energy production target of 1000 MWh was set for each of the four main regions. This ensures not only that high-potential areas contribute to total production but also that generation is spatially distributed to support energy security. The regional structure aids in balancing the grid, encourages equitable utilization of local capacity, and facilitates effective clustering of wind turbines.

Minimum turbine spacing and cell definition: To prevent wake effects and enhance aerodynamic efficiency, a rectangular area corresponding to 60 meters in the horizontal direction and 100 meters in the vertical direction was defined as a "cell." All placement calculations in the model were conducted based on these cells.

3.2.6. Determination of the Noise Level Limit

During the operation of wind turbines, components such as rotor blades, the generator, and the gearbox generate noise, which is an important parameter that must be considered, particularly for turbines installed near residential areas. In this study, the noise levels of the turbine types were obtained from manufacturer catalogues and are presented in Table 4.

While defining the candidate regions, the criterion “distance to protected areas” was used, and only locations at least 2000 meters away from such areas were selected. This ensured that noise pollution and other environmental impacts associated with wind turbines were minimized to levels acceptable for human health and living comfort. According to the literature, turbine-generated noise decreases with increasing distance. The World Health Organization (WHO) and EU directives recommend limiting wind turbine noise near residential areas to below 45 decibels (dB) (WHO, 2018). Therefore, this study aimed to ensure that the noise level at a distance of 2000 meters does not exceed the 45 dB threshold.

The dB unit Is a logarithmic measure of sound and can be converted into the physical quantity of sound intensity (W/m²) as shown in Equation (5) (Rossing, 2007):

$$I = I_0 \cdot 10^{\frac{L_p}{10}} \tag{5}$$

where I represents the sound intensity (W/m²), I_0 is the reference sound intensity (10^{-12} W/m²), and L_p is the sound pressure level (dB).

For a sound level of 45 dB, the corresponding intensity is calculated as: $I = 3.16 \times 10^{-8}\ \mathrm{W/m^2}$.

Assuming that sound energy is radiated spherically into the environment, the total acoustic power at a given distance can be computed using Equation (6):

$$P = I \cdot 4\pi r^2 \tag{6}$$

where P is the total sound power (W), I is the previously calculated intensity, and r is the radius of propagation (m). Using r=2000 m, the maximum total acoustic power corresponding to 45 dB is: $P = 1.58$ W. Accordingly, the average power intensity at this distance is: $\frac{P}{4\pi r^2} = 1.58 \times 10^{-6}\ \mathrm{W/m^2}$. In this study, a more conservative approach was adopted, and the noise limit was set even lower, at: $1 \times 10^{-6}\ \mathrm{W/m^2}$ ensuring an additional safety margin for environmental and human health considerations.

3.2.7. Emission Limit Determination

In the model, it is aimed to constrain the total carbon emissions generated per unit of electricity produced by the wind turbines. For this purpose, the carbon footprint values provided in the manufacturer catalogues (expressed as CO_2e/kWh for each turbine type) were integrated into the model.

Table 8: Electricity generation emission factors for Türkiye

Fuel Type	Value (tCO_2/MWh)	Value (tCO_2-eq./MWh)
Lignite	1.177	1.188
Hard coal	1.007	1.011
Asphaltite	1.019	1.024
Imported coal	0.816	0.820
Natural gas	0.374	0.379
Fuel oil	1.310	1.312
Diesel	0.947	0.948

Reference: T.C. Ministry of Energy and Natural Resources, 2022

Based on the data published by the Ministry of Energy and Natural Resources (2022), Table 8 presents the average greenhouse gas emission factors per unit of electricity generation for various fuel types used across Türkiye, expressed in terms of CO_2 and CO_2 equivalent (CO_2e). Among fossil-based options, natural gas exhibits the lowest emission factor. To enhance the model's alignment with sustainability principles, the emission level of natural gas–based electricity production was adopted as the reference value, and an upper limit corresponding to only 1% of this value was imposed. In this way, the total emissions associated with wind turbine operation are constrained to remain significantly below even the least carbon-intensive conventional generation technology, thereby reinforcing the principle of near-zero-carbon electricity production.

The defined emission limit was evaluated separately for the four main regions. The corresponding constraints ensure that, for each region,

the total emissions associated with all installed turbines do not exceed the specified upper threshold relative to their total electricity output.

3.2.8. Regional Capacity Constraint

In the model, a maximum installed capacity limit was defined for each region. This limit was determined to prevent the technical capacity of transformer substations from being exceeded and was calculated for each region using a capacity density coefficient based on the area size. Numerous studies on wind energy projects indicate that the average capacity density associated with land use ranges between 1.0 and 11.2 MW/km², with most values concentrated between 2 and 10 MW/km² (Denholm et al., 2009). Accordingly, considering recent technological advancements that have improved turbine efficiency and optimized land use, a capacity density of 10 MW/km² was adopted.

The selected capacity density coefficient was multiplied by the area of each region to determine its maximum allowable installed capacity. In this way, turbine placement was ensured to remain within the physical capacity constraints of each regional cluster, thereby maintaining compliance with substation capacity limitations and preventing excessive turbine concentration within any region.

3.2.9. Turbine Placement Area Calculations

The width *(W(k)), height (H(k))*, *X* and *Y* coordinates, and the distance to the nearest substation *(l(k))* for each region were obtained through GIS analysis and presented earlier in Table 3. In the model, instead of

using the total area directly, the width and height values defined according to a rectangular layout were taken as the primary basis. The main rationale behind this approach is to establish a rational and non-overlapping grid structure that maintains the minimum horizontal and vertical separation distances required between turbines.

Accordingly, each region was divided into grid cells of 60 × 100 meters, and the number of cells required for each turbine type was calculated based on the area occupied by the turbine determined by its rotor diameter. Letting s_h=60 and s_v=100 m represent the horizontal and vertical grid cell dimensions, the maximum turbine placement capacity for each region—expressed in cell units—is computed using Equation (7):

$$\text{Maximum number of cells}(k) = \left\lfloor \frac{W_k}{s_h} \right\rfloor \cdot \left\lfloor \frac{H_k}{s_v} \right\rfloor \tag{7}$$

The area occupied by each turbine within this grid structure is determined based on its rotor diameter and is calculated using Equation (8):

$$\text{Area per turbine}(t) = \left\lceil \frac{H_u(t)}{s_h} \cdot \frac{V_u(t)}{s_v} \right\rceil \tag{8}$$

Here, $H_u(t)$ and $V_u(t)$ denote the required horizontal and vertical spacing between turbines, respectively, which are based on the rotor diameter D_t and computed using Equations (9) and (10):

$$H_u(t) = R_H \cdot D_t \tag{9}$$

$$V_u(t) = R_V \cdot D_t \quad (10)$$

A spacing of three rotor diameters horizontally and five rotor diameters vertically was adopted, and therefore the constant coefficients R_H and R_V were set to 3 and 5, respectively. The resulting cell requirements calculated using Equations (8)–(10) were rounded up and are presented in Table 9.

Table 9: Cell Requirements for Turbine Types

Turbine Type	Model Name	Rotor Diameter (m)	Required Area (m^2)	Required Number of Cells (calculated)	Required Number of Cells (rounded up)
t1	RPWM	75	84,375	14.06	15
t2	VST1	90	121,500	20.25	21
t3	VST2	110	181,500	30.25	31
t4	VST3	100	150,000	25.00	25
t5	VST4	116	201,840	33.64	34
t6	VST5	120	216,000	36.00	36
t7–t8	VST6 / VST7	117	205,335	34.22	35
t9	VST8	126	238,140	39.69	40
t10–t11–t12	VST9 / VST10 / VST11	136	277,440	46.24	47
t13–t14–t16	VST12 / VST13 / VST15	150	337,500	56.25	57
t15	VST14	163	398,535	66.42	67
t17–t18	VST16 / VST17	162	393,660	65.61	66
t19	VST18	172	443,760	73.96	74

This approach ensures that the turbine capacity of each region is calculated not only based on the physical land area but also according to grid-based placement feasibility, thereby enhancing the practical

applicability of the model.

3.2.10. Energy Efficiency Loss Factor Calculation

Energy losses occurring along transmission lines during the transfer of electricity generated by wind turbines to transformer substations constitute an important factor influencing the overall system efficiency (Ackermann, 2005). Therefore, the model incorporates a correction coefficient that approximately accounts for these losses for each region. The efficiency loss coefficient η_k is defined as a function of the distance of each region to the nearest substation and is expressed by Equation (11):

$$\eta_k = 1 - 0{,}00001 \cdot l(k) \tag{11}$$

Here, $l(k)$ denotes the distance (in meters) from region k to the nearest transformer substation. According to the formula, efficiency decreases as the distance to the substation increases. This linear reduction represents a simplified approximation of technical factors encountered in electricity transmission, such as line resistance, conversion losses, and maintenance conditions. By incorporating this coefficient into the model, not only the theoretical production based on installed capacity and capacity factor but also the effectively deliverable amount of energy is taken into account, thereby enabling a more realistic planning approach.

3.2.11. Determination of the Energy Production Target

One of the fundamental parameters of the model is the annual energy production target, which was determined in alignment with regional energy consumption levels, national trends, and Türkiye's policy objectives. Table 10 presents the distribution of Türkiye's electricity generation by source for the year 2023 (Turkish Electricity Transmission Corporation, 2025). According to Table 10, wind energy contributed 34,109.05 GWh, corresponding to 10.3% of Türkiye's total electricity production.

Table 10: Distribution of Türkiye's Electricity Generation by Source in 2023

Source	Generation (GWh)	Contribution (%)
Imported Coal	72,719.40	21.96
Hard Coal + Asphaltite	5,341.69	1.61
Lignite	41,735.31	12.60
Natural Gas	69,452.23	20.97
Liquid Fuels	471.42	0.14
Reservoir Hydropower	44,302.17	13.38
Run-of-River and Canal Hydropower	19,700.28	5.95
Wind	34,109.05	10.30
Renewable + Waste + Waste Heat	10,124.73	3.06
Geothermal	11,102.08	3.35
Solar	22,090.56	6.67

Reference: Turkish Electricity Transmission Corporation, 2025

In Table 11, the installed capacity and electricity generation by province are presented (Energy Atlas, 2025). According to Table 11, the annual electricity consumption per province in Türkiye is calculated as approximately 4,110,383 MWh, while the annual total

electricity consumption of Kocaeli is 14,768,000 MWh. This indicates that Kocaeli has a significantly higher electricity demand compared to the national average and occupies a strategic position within Türkiye due to its high level of industrial activity.

In determining the energy production target, the national share of wind energy in Türkiye's total electricity generation was taken as the reference.

Table 11: Installed Capacity and Electricity Consumption by Province

Province	Installed Capacity (MW)	Consumption (MWh)	Province	Installed Capacity (MW)	Consumption (MWh)	Province	Installed Capacity (MW)
İstanbul	3,746	53,703,000	Mardin	1,455	3,105,000	Yalova	407
İzmir	5,515	21,314,000	Bilecik	327	3,057,000	Nevşehir	260
Ankara	3,147	19,063,000	Afyonkarahisar	705	2,701,000	Yozgat	168
Bursa	3,119	16,612,000	Uşak	364	2,657,000	Rize	353
Kocaeli	2,260	14,768,000	Kütahya	1,198	2,451,000	Giresun	963
Gaziantep	1,024	11,434,000	Malatya	243	2,359,000	Karabük	215
Antalya	2,081	11,256,000	Sivas	1,110	2,008,000	Erzincan	372
Adana	5,456	10,218,000	Trabzon	663	2,005,000	Şırnak	453
Konya	2,513	10,089,000	Ordu	508	1,805,000	Amasya	365
Tekirdağ	1,570	9,726,000	Elazığ	2,508	1,769,000	Kırıkkale	2,079
Şanlıurfa	3,592	8,287,000	Niğde	464	1,760,000	Çankırı	166
Hatay	2,946	7,069,000	Adıyaman	403	1,697,000	Kilis	49
Mersin	1,376	6,875,000	Zonguldak	3,421	1,614,000	Ağrı	74
Manisa	3,280	6,162,000	Aksaray	189	1,606,000	Siirt	802
Osmaniye	1,233	5,799,000	Bolu	504	1,538,000	Kırşehir	414

Province	Installed Capacity (MW)	Consumption (MWh)	Province	Installed Capacity (MW)	Consumption (MWh)	Province	Installed Capacity (MW)
Sakarya	2,944	5,444,000	Kastamonu	163	1,489,000	Artvin	2,363
Kahramanmaraş	4,780	5,435,000	Düzce	143	1,465,000	Muş	481
Kayseri	1,230	5,428,000	Van	269	1,430,000	Gümüşhane	670
Balıkesir	3,331	4,960,000	Edirne	234	1,381,000	Bitlis	90
Denizli	2,011	4,929,000	Isparta	548	1,367,000	Sinop	629
Muğla	2,442	4,772,000	Karaman	869	1,291,000	Kars	258
Samsun	3,081	4,590,000	Burdur	246	1,254,000	Bingöl	1,636
Eskişehir	799	4,367,000	Batman	85	1,249,000	Hakkari	67
Diyarbakır	2,432	4,087,000	Erzurum	931	1,210,000	Iğdır	26
Çanakkale	4,743	3,967,000	Çorum	567	1,179,000	Tunceli	108
Aydın	1,778	3,925,000	Tokat	729	1,175,000	Ardahan	240
Kırklareli	1,937	3,442,000	Bartın	49	1,151,000	Bayburt	83

Based on Türkiye's average share of 10%, an annual production target of approximately 411,038 MWh is proposed. This amount corresponds to only 2.78% of Kocaeli's total electricity consumption. Given Kocaeli's high energy demand and industrial load, this proportion may be insufficient from a wind energy planning perspective. Therefore, it was deemed necessary to establish a higher production target for Kocaeli, and scenarios within the range of 10% to 20% were considered. As shown in Table 12, this range corresponds to approximately 2.78% to 5.57% of Kocaeli's total electricity consumption.

Table 12: Determination of the Energy Production Target

Annual Production Amount (MWh)	Share of Türkiye's Average Consumption (%)	Share of Kocaeli's Average Consumption (%)
411,038.27	10.00%	2.78%
452,142.10	11.00%	3.06%
493,245.93	12.00%	3.34%
534,349.75	13.00%	3.62%
575,453.58	14.00%	3.90%
616,557.41	15.00%	4.17%
657,661.23	16.00%	4.45%
698,765.06	17.00%	4.73%
739,868.89	18.00%	5.01%
780,972.72	19.00%	5.29%
822,076.54	20.00%	5.57%

3.2.12. Calculation of Total Energy Production

The total amount of energy produced over the economic lifetime of the system is calculated based on the annual energy production coefficient $\delta(a)$, as defined in Equation (12). This coefficient represents the annual 0.5% performance degradation that occurs in wind turbines over time. Equation (12) cumulatively computes the total energy generated throughout the system's operational life and serves as a key model output.

$$\text{Total energy production} = \sum_a \delta(a) \cdot \sum_k \sum_t \eta_k \cdot P_t \cdot CF_t \cdot 8760 \cdot n_{kt} \quad (12)$$

3.2.13. Formulation of the Model

The mathematical model developed for the site selection and capacity planning of onshore wind turbines aims to minimize the total system

cost. Table 13 provides the symbols used in the model along with their corresponding definitions.

Table 13: Symbols and Their Descriptions

Symbol	Description
k	Set of regions (k_1, k_2, …, k_{41})
R_j	Set of primary energy sub-regions (j_1, j_2, j_3, j_4)
t	Set of turbine types (t_1, t_2, …, t_{19})
a	Set of years (a_1, a_2, …, a_{25})
n_{kt}	Number of turbines of type t installed in region k
y_k	Binary variable indicating whether turbines are installed in region k
Z	Objective function minimizing total system cost over the economic lifetime
K_t	Installation cost of a turbine of type t ($)
B_t	Annual maintenance cost of a turbine of type t ($)
V_t	Annual variable operational cost of a turbine of type t ($)
L	Economic lifetime of turbines (years)
$l(k)$	Distance from region k to the nearest transformer substation (m)
c	Unit cost of energy transmission ($/m)
η_k	Efficiency loss coefficient for region k
P_t	Power capacity of turbine type t (MW)
CF_t	Capacity factor of turbine type t
S_k	Total area of region k (m^2)
A_j	Total land area of energy sub-region j (km^2)
Ca	Unit land cost ($/$m^2$)
H_t	Scrap value of a turbine of type t ($)
E	Annual energy production target (MWh)
$d_{kk'}$	Euclidean distance between regions k and k' (m)
H_k	Maximum number of grid cells available for placement in region k

Symbol	Description
h_t	Number of grid cells required by a turbine of type *t*
N_{maks}	Maximum allowable number of turbines
n_{min}	Minimum number of turbines required for each installed region
Ca_{maks}	Total budget allocated for land acquisition ($)
E_j^{min}	Minimum required production for each primary energy sub-region *j* (MWh)
D_{min}	Minimum required distance between any two regions with turbine installation (m)
SP_t	Sound power level of turbine type *t* (W)
SP_{maks}	Maximum allowable sound power per unit area (W/m²)
FP_t	Carbon footprint of turbine type *t* (gCO_2e/kWh)
ε_{maks}	Maximum emission limit per unit of electricity produced (tCO_2e/MWh)
Cap_j^{maks}	Maximum installed capacity limit for primary energy sub-region *j* (MW)
ρ	Capacity density coefficient (MW/km²)
i	Discount rate
λ	Annual degradation (production loss) rate
$\delta(a)$	Production efficiency coefficient in year *a*
$g(a)$	Cost escalation coefficient in year *a*
C_y	Balance-of-plant cost per turbine
C_b	Maintenance-equipment cost per turbine
C_g	Project development cost per MW
C_l	Licensing cost per MW
C_d	Other fixed cost per turbine
C_m	Annual salary of security personnel ($)
N_k^p	Number of personnel employed in region *k*

The objective function presented in Equation (13) aims to minimize the total cost incurred over the economic lifetime of the onshore wind

turbine system. This function accounts for several cost components for each turbine type, including installation costs, balance-of-plant expenditures, maintenance-equipment costs, project development and licensing costs. In addition, annual maintenance costs, variable operational costs, energy transmission costs based on distance to substations, and other fixed expenses are incorporated each year according to the annual cost escalation coefficient. Furthermore, land-use costs in the regions where turbines are installed as well as annual salaries of security personnel assigned to these regions are included as part of the annually increasing expenses. While all these cost items are added to the total cost on a yearly basis, the salvage value recovered from turbines at the end of their economic lifetime is discounted to its present value using the discount rate and subtracted from the total cost. In this way, the model evaluates system costs by incorporating dynamic cost changes over time and long-term investment returns.

$$\min Z = \sum_k \sum_t \left[K_t + C_y + C_b + C_g \cdot P_t + C_l \cdot P_t + \sum_{a=1}^{L} g(a) \cdot \right.$$
$$\left.(B_t + V_t + c \cdot l(k) \cdot \lambda_k \cdot CF_t \cdot P_t \cdot 8760 + C_d)\right] \cdot n_{kt} + \sum_{a=1}^{L} g(a) \cdot$$
$$\left(\sum_k y_k \cdot S_k \cdot Ca + \sum_k N_k^p \cdot C_m\right) - \sum_k \sum_t \frac{H_t}{(1+i)^L} \cdot n_{kt} \qquad (13)$$

The model is solved subject to the following constraints:

Minimum initial energy production constraint: According to the constraint expressed in Equation (14), the minimum production target must be satisfied by the end of the first year. Annual production is calculated by considering the nominal turbine power, capacity factor,

and efficiency loss coefficient. Only first-year production is included here, while year-by-year changes are handled separately through Equation (12).

$$\sum_k \sum_t \eta_k \cdot P_t \cdot CF_t \cdot 8760 \cdot n_{kt} \geq E_h \quad (14)$$

Installation decision constraints: The binary decision variable y_k is linked to the number of turbines installed in each region. Equation (15) ensures that if no installation takes place in region k (i.e., y_k=0), then no turbine can be placed there. Conversely, if y_k=1, up to M turbines may be installed in that region. Equation (16) ensures that, if installation occurs, a meaningful minimum number of turbines must be installed.

$$\sum_t n_{kt} \leq M \cdot y_k \quad \forall k \quad (15)$$

$$\sum_t n_{kt} \geq n_{min} \cdot y_k \quad \forall k \quad (16)$$

Total number of turbines constraint: The constraint in Equation (17) ensures that the total number of turbines installed across all regions does not exceed a predefined upper limit.

$$\sum_k \sum_t n_{kt} \leq N_{max} \quad (17)$$

Land cost constraint: The land cost constraint defined in Equation (18) aims to control the total economic burden associated with land used in regions where turbine installation takes place. In the model, if at least one turbine is installed in region k, it is assumed that the entire area of that region is utilized. Accordingly, the total land cost for

region k is calculated by multiplying its total area S_k by the unit land cost Ca. The sum of these costs across all regions must not exceed the total land budget $Ca_{\max}$ specified by the decision maker. In this way, land-related investment expenditures are kept within sustainable limits.

$$\sum_k y_k \cdot S_k \cdot Ca \leq Ca_{max} \quad (18)$$

Region-based cell capacity constraint: The constraint expressed in Equation (19) is introduced to ensure that the physical placement capacity defined for each region k is not exceeded. Here, h_t denotes the number of grid cells required by a turbine of type t, while H_k represents the total number of available cells in region k. Thus, the total cell usage within a region is restricted so that it does not exceed the region's physical capacity. This constraint ensures a realistic geographical distribution of turbines and prevents excessive concentration.

$$\sum_t n_{kt} \cdot h_t \leq H_k \quad \forall k \quad (19)$$

Minimum energy production constraints for regional clusters: To ensure a balanced supply of regional energy, the potential sites are grouped into primary energy clusters R_j, and minimum production targets are defined for each cluster. According to the constraint presented in Equation (20), the total energy generated in the first year by all regions within cluster R_j must meet or exceed the threshold value E_j^{min}. The production quantity is computed by multiplying the

turbine's rated capacity P_t, capacity factor CF_t, efficiency loss coefficient η_k, and the number of hours in a year (8760), and then summing across all regions and turbine types. This constraint ensures not only compliance with total production requirements but also the attainment of geographical equity and energy supply security across clusters.

$$\sum_{k \in R_j} \sum_t \eta_k \cdot P_t \cdot CF_t \cdot 8760 \cdot n_{kt} \geq E_j^{min} \quad \forall j = 1,2,3,4 \tag{20}$$

Inter-regional distance constraint: The constraint defined in Equation (21) imposes a minimum separation distance D^{min} between turbine installation regions. The objective is to prevent physical overlap of rotor areas, reduce wake-induced turbulence effects, and ensure safe access conditions for maintenance. Accordingly, if the Euclidean distance $d_{kk'}$ between two regions k and k' is smaller than the specified minimum threshold, turbines cannot be installed in both regions simultaneously. This constraint plays a decisive role particularly in cases where potential sites are spatially close to each other.

$$y_k + y_{k'} \leq 1 \quad \text{if } d_{kk'} < D^{min} \tag{21}$$

Noise level constraint: The noise constraint presented in Equation (22) ensures that the total sound power generated by turbines installed in each region does not exceed the maximum allowable sound power per unit area, denoted as SP_{max}. The total noise level in region k is obtained by multiplying the sound power of each turbine type SP_t by

the corresponding number of installed turbines. This total must remain below the limit defined by $SP_{\max}$. S_k, where S_k is the area of region k. Through this formulation, the model controls the areal noise intensity based on turbine density and land area.

$$\sum_t SP_t \cdot n_{kt} \leq SP_{max} \cdot S_k \quad \forall k \tag{22}$$

The sound power level SP_t for turbine type t, based on the sound pressure level $L_{p,t}$ in decibels, is computed using Equation (23):

$$SP_t = I_0 \cdot 10^{L_{p,t}/10} \cdot 4\pi r^2 \tag{23}$$

Carbon emission constraint: The carbon footprint constraint shown in Equation (24) is defined separately for each primary energy cluster R_j. These constraints ensure that the annual greenhouse gas emissions associated with wind turbine operation do not exceed the maximum allowable emission intensity $\varepsilon_{\max}$, determined relative to the production level of each cluster. For each turbine type, the annual emission amount is calculated by multiplying its carbon footprint per unit of electricity produced FP_t by the installed capacity, capacity factor, annual hours (8760), and efficiency coefficient η_k. This value is then divided by 10^6 to convert from grams to metric tons of CO_2 equivalent. The total emission for cluster R_j must not exceed the product of the cluster's total energy production and the maximum emission intensity limit.

$$\sum_{k\in R_j}\sum_t CF_t \cdot P_t \cdot n_{kt} \cdot 8760 \cdot \eta_k \cdot \frac{FP_t}{10^6} \leq \varepsilon_{max} \cdot \sum_{k\in R_j}\sum_t CF_t \cdot P_t \cdot n_{kt} \cdot 8760 \cdot \eta_k \quad (24)$$

This regional implementation supports geographical sustainability principles and ensures equitable spatial distribution of environmental impacts.

Installed capacity constraint: The constraint defined in Equation (25) ensures that the total wind turbine capacity installed within each primary energy region does not exceed the maximum allowable installed capacity, which is calculated based on the physical size of the region. For each energy cluster R_j, the maximum installable capacity is obtained by multiplying the capacity density coefficient ρ by the total area A_j, as shown in Equation (26). The total installed capacity is calculated by multiplying the rated power of each turbine type P_t by the number of turbines installed in each region. This constraint guarantees compliance with the technical capacities of transformer substations and ensures a balanced spatial distribution of turbines across available land.

$$\sum_{k\in R_j}\sum_t P_t \cdot n_{kt} \leq Cap_j^{max} \quad \forall j \quad (25)$$

$$Cap_j^{max} = \rho . A_j \quad (26)$$

Non-negativity and binary constraints: Finally, to ensure that the decision variables take meaningful and implementable values, non-negativity and integrality constraints are imposed. The variable n_{kt},

representing the number of turbines of type t installed in region k, is restricted to take only non-negative integer values. The binary variable y_k, which indicates whether turbine installation occurs in region k, can take only the values 0 or 1. These constraints are expressed in Equations (27) and (28).

$$n_{kt} \geq 0, \quad n_{kt} \in Z, \quad \forall k, \forall t \tag{27}$$

$$y_k \in \{0,1\}, \quad \forall k \tag{28}$$

3.3. Model Solution

The mathematical model defined above does not contain any nonlinear components; however, since the decision variables include both integer and binary terms, the problem was solved using Mixed Integer Linear Programming (MILP). The model was implemented and solved in GAMS Studio version 49.0 using the CPLEX solver. Multiple model runs were performed under different energy production target scenarios, and a sensitivity analysis was conducted based on these scenarios. For each scenario, installation decisions at the regional level, selected turbine types, and total investment costs were analyzed separately, allowing the impact of the energy target on model outputs to be systematically evaluated.

In Table 12, eleven different annual energy production targets were defined based on the percentage distribution of Türkiye's average electricity consumption. The regional turbine types and quantities

corresponding to the first seven of these targets are presented in Tables 14, 15, 16, 17, 18, 19, and 20, respectively.

Table 14: Turbine Types and Quantities by Region for 411,038.27 MWh

Region	t1	t3	t7	t15
k2	1			
k25				18
k33		1	1	1
k40	1			

Table 15: Turbine Types and Quantities by Region for 452,142.10 MWh

Region	t1	t3	t5	t15
k2	1			
k25			1	19
k33		1	1	1
k38				1

Table 16: Turbine Types and Quantities by Region for 493,245.93 MWh

Region	t1	t4	t5	t6	t7	t15
k2	1					
k25			1	1	5	17
k33		1			3	
k38						1

Table 17: Turbine Types and Quantities by Region for 534,349.75 MWh

Region	t1	t3	t4	t7	t15
k2	1				
k25				7	17
k33			1	3	
k38		1		1	
k39			1	2	

Table 18: Turbine Types and Quantities by Region for 575,453.58 MWh

Region	t1	t3	t4	t7	t15
k2	1				
k24		1			1
k25		1		10	15
k26		1			
k33			1	3	
k38					1
k39			1	2	

Table 19: Turbine Types and Quantities by Region for 616,557.41 MWh

Region	t1	t3	t4	t5	t7	t15
k2	1					
k9		1				
k24			1		2	
k25		1			10	15
k29				1	2	
k33			1		3	
k38		1			1	
k39			1		2	

Table 20: Turbine Types and Quantities by Region for 657,661.23 MWh

Region	t1	t2	t3	t4	t5	t6	t7	t9	t15
k2	1								
k9	2								
k10		1							
k20								1	
k23							6		
k25						1			20
k29					1		2		
k33				1			3		
k38			1				1		
k39				1			2		

Under the current set of constraints, the next target level of 698,765.06 MWh of annual energy production could not be achieved. In this study, candidate locations for WPP deployment were identified based on GIS analyses by considering only those areas with a wind energy suitability score of 23 or higher. However, it should be noted that if this threshold were lowered to the 20–22 range, reaching the remaining production targets might become feasible. Based on the conducted analyses, the maximum achievable first-year energy production specific to this model was calculated as 691,620 MWh. This amount corresponds to approximately 4.68% of Kocaeli's total electricity consumption. Considering that Kocaeli's energy demand is significantly higher than the national average, the same production level corresponds to approximately 16.83% relative to Türkiye's average provincial consumption. When evaluated in the context of Türkiye's existing share of wind energy in installed capacity and its technical potential, this proportion may be regarded as reasonable. The

matrix presenting the turbine types and quantities installed across regions for this production level is provided in Table 21.

Table 21: Turbine Types and Quantities by Region for 691,620 MWh

Region	t1	t2	t3	t4	t5	t6	t7	t9	t10	t15
k6	1									
k9	2									
k10		1								
k20								1		
k23										3
k24						1			1	
k25					1					20
k26			1							
k28				1						
k29							1			1
k32								1		
k33			1				1			1
k38										1
k39			1							1
k40	1									
k41	1									

Table 21 presents a comparative summary of the model results obtained under different energy production targets.

In accordance with Presidential Decree No. 7189 published in the Official Gazette dated 1 May 2023 and numbered 32177, the updated unit prices applicable to renewable energy generation facilities holding a Renewable Energy Certificate (YEK Certificate) and commissioned between 1 July 2021 and 31 December 2030 are announced periodically under the support mechanism. As of 1 May 2025, the YEKDEM unit price, including the domestic manufacturing support, has been set at 2.7244 TRY/kWh (0.07 USD/kWh) (EPİAŞ,

2025). Based on the designated sales price, the investment's payback period has been calculated and is presented in Table 22.

Table 21: Comparison of Results Across Different Energy Production Targets

	Model 1	**Model 2**	**Model 3**	**Model 4**
Target energy (MWh)	411,038.27	452,142.10	493,245.93	534,349.75
Objective function ($)	2,297,600,817.20	2,439,017,601.40	2,601,741,420.72	2,817,510,415.72
Annual average cost ($/year)	91,904,032.69	97,560,704.06	104,069,656.83	112,700,416.63
Total salvage value ($)	2,984,152.80	3,288,248.32	3,947,746.47	4,431,248.58
Total number of turbines	23	25	30	34
Number of installed regions	4	4	4	5
First-year energy production (MWh/year)	411,445.10	452,614.10	493,271.54	534,918.86
Lifetime energy production (MWh)	9,691,980.74	10,661,756.00	11,619,480.00	12,600,520.00
	Model 5	**Model 6**	**Model 7**	**Model 8**
Target energy (MWh)	575,453.58	616,557.41	657,661.23	691,620.00
Objective function ($)	3,081,882,560.03	3,375,705,081.08	3,721,370,532.16	4,103,726,975.98
Annual average cost ($/year)	123,275,302.40	135,028,203.24	148,854,821.29	164,149,079.04
Total salvage value ($)	4,899,703.66	5,526,738.30	5,659,118.77	5,640,065.00

Table 22: Calculation of Investment Payback Periods

	Model 1	**Model 2**	**Model 3**	**Model 4**
Total revenue ($)	678,438,651.80	746,322,920.00	813,363,600.00	882,036,400.00
Total cost ($)	2,297,600,817.20	2,439,017,601.40	2,601,741,420.72	2,817,510,415.72
Payback ratio (years)	3.386600706	3.268045957	3.198743367	3.194324424
Payback period (months)	40.63920847	39.21655149	38.38492041	38.33189309
Approximate payback period (months)	41	40	39	39
	Model 5	**Model 6**	**Model 7**	**Model 8**
Total revenue ($)	949,926,600.00	1,016,694,000.00	1,084,557,600.00	1,140,423,900.00
Total cost ($)	3,081,882,560.03	3,375,705,081.08	3,721,370,532.16	4,103,726,975.98
Payback ratio (years)	3.244337573	3.320276387	3.431233650	3.598422460
Payback period (months)	38.93205088	39.84331664	41.17480380	43.18106952
Approximate payback period (months)	39	40	42	44

According to Table 22, the investment payback period ranges between 39 and 44 months. In several pre-feasibility reports for wind WPPs, the payback period is typically reported as 8–10 years. However, in real-world applications, a substantial portion of the investment is usually financed through loans, while the share of equity capital remains limited. This significantly increases financial costs, as loans involve additional components such as interest burdens and maturity differences. Moreover, while loan repayments are generally made through fixed periodic installments, revenues generated by the power plant may fluctuate due to seasonal variations in energy production.

Additionally, various external factors such as exchange rate risks during turbine procurement and construction, insurance expenses, bureaucratic challenges encountered during the licensing process, and investments required for grid connection infrastructure can also affect cash flows and extend the payback period. Since the payback durations calculated in this study are based on ideal conditions that do not incorporate financial risks, managerial uncertainties, or market fluctuations, the resulting payback periods are reasonably lower. The LCOE values for the models are presented in Table 23.

Table 23: Determination of LCOE

	Total Cost ($)	Total Production (kWh)	YEKDEM Revenue ($)	Net Cost ($)	Net LCOE ($/kWh)
Model 1	2.297.600.817,20	9.691.980.740	678.438.651,80	1.619.162.165,40	0,1671
Model 2	2.439.017.601,40	10.661.756.000	746.322.920,00	1.692.694.681,40	0,1588
Model 3	2.601.741.420,72	11.619.480.000	813.363.600,00	1.788.377.820,72	0,1539
Model 4	2.817.510.415,72	12.600.520.000	882.036.400,00	1.935.474.015,72	0,1536
Model 5	3.081.882.560,03	13.570.380.000	949.926.600,00	2.131.955.960,03	0,1571
Model 6	3.375.705.081,08	14.524.200.000	1.016.694.000,00	2.359.011.081,08	0,1624
Model 7	3.721.370.532,16	15.493.680.000	1.084.557.600,00	2.636.812.932,16	0,1702
Model 8	4.103.726.975,98	16.291.770.000	1.140.423.900,00	2.963.303.075,98	0,1819

According to data published by IRENA for the year 2019, the LCOE for onshore wind energy projects in the European region ranges between 0.037 USD/kWh and 0.096 USD/kWh. When the LCOE values obtained from the eight models developed in this study are

examined, it is observed that the results are slightly above this range (IRENA, 2020). However, IRENA's reported LCOE values predominantly reflect large-scale projects that benefit from economies of scale and public incentives. As a result, the dataset is weighted toward relatively low-cost projects, which leads to lower average LCOE levels.

In contrast, the models analyzed in this study incorporate several local factors such as limited site capacity, turbine-type diversity, energy transmission costs, and infrastructure expenditures. Furthermore, for annual operation and maintenance costs of onshore wind farms, the highest value reported by IRENA based on the 2016–2018 period was adopted in this study, resulting in comparatively conservative cost assumptions. In this context, the relatively high LCOE values reaching up to 0.18 USD/kWh in more complex installation scenarios such as Model 8 are technically and economically reasonable. Therefore, it can be concluded that the LCOE outcomes obtained in this study are consistent with IRENA's data when the underlying methodological and contextual differences are taken into account.

4. CONCLUSION AND DISCUSSION

Climate change, increasing energy demand, and the environmental pressures associated with fossil fuels compel countries to develop sustainable and long-term energy policies. In this context, the effective planning of renewable energy resources and the use of scientifically grounded decision-support models have become strategic necessities

not only from an environmental perspective but also from economic and social standpoints. Considering Türkiye's diverse geographical, climatic, and socioeconomic characteristics, it is evident that a single national framework is insufficient for energy planning; rather, analytical models that incorporate regional differences are indispensable. Building upon this need, the present study aims to develop a comprehensive decision-support system integrating GIS and mathematical optimization techniques.

Kocaeli, characterized by its large population, strong industrial infrastructure, and electricity consumption levels significantly above the national average, stands as one of Türkiye's most critical provinces in terms of energy demand. This situation necessitates placing Kocaeli at the forefront of energy supply security planning and prioritizing sustainable energy investments. Wind energy emerges as a suitable option for such high-demand regions due to its high reliability and operational continuity.

Accordingly, the study first conducted a detailed GIS-based site-selection analysis. Multiple spatial criteria— including elevation, wind speed, wind power density, capacity factor, proximity to water bodies, fault lines, transmission lines, road networks, and protected areas—were jointly evaluated. The spatial layers were equally weighted, and an overlay analysis was performed, resulting in suitability scores ranging from 0 to 25.5 for each grid cell. Regions with a score of 23 or higher were designated as candidate WPP sites. Selecting such threshold values ensured a decision space that was both

meaningful and manageable. High-suitability regions were converted from raster to vector format, digitized as independent polygons, and their geometric characteristics and distances to the nearest substations were computed.

Based on these data, a MILP model was developed to determine the minimum cost placement of onshore wind turbines across the candidate regions. The structure of the model integrates multiple dimensions including turbine technical characteristics, investment and operating costs, energy production targets, regional balance, and environmental sustainability within a unified analytical framework. In this regard, the model offers a scalable decision-support tool that may be applied to other provinces with similar characteristics.

The 19 turbine types incorporated into the model were selected from internationally recognized manufacturer catalogues, and their annual energy outputs were estimated based on the production values corresponding to a reference wind speed of 7.5 m/s. Scrap values were computed using the methodology of Şentürk and Oğuz (2020) and discounted to 2025 price levels. The economic lifetime of turbines was set at 25 years, with annual efficiency losses assumed at 0.5%, and maintenance, operating, and security costs growing at 7.5% annually. Energy transmission costs were incorporated based on each region's distance to the nearest substation.

The objective function of the model minimizes the total cost over the system's economic lifetime. The 41 candidate regions identified

through GIS were grouped into four main clusters, and minimum production targets were assigned to each, ensuring geographical equity and energy supply security. A 60 × 100 m grid-based layout was adopted to avoid spatial overlap, and horizontal and vertical turbine spacing requirements were defined based on rotor diameter. A minimum inter-region distance constraint was also implemented. Furthermore, environmental sustainability was incorporated via a noise constraint consistent with the WHO guideline of 45 dB and a carbon intensity constraint defined as 1% of the emission value of natural gas-based electricity generation.

The LCOE values obtained from the eight scenario models were slightly above IRENA's (2020) reported range of 0.037–0.096 USD/kWh for onshore wind projects in Europe. However, IRENA's figures predominantly represent large-scale, incentive-supported projects that benefit from economies of scale. In contrast, the models in this study incorporate limited installation capacity, turbine diversity, transmission-distance-based costs, and conservative operating cost assumptions. For this reason, LCOE values as high as 0.18 USD/kWh in more complex scenarios such as Model 8 are technically and economically reasonable.

There remain several avenues for enhancing the model in future research. Although transformer capacity limitations were indirectly captured through regional constraints, incorporating transformer-based capacity allocations directly into the model would allow for more precise transmission planning. The assumption that all regions share

homogeneous cost structures does not fully reflect the logistical challenges imposed by different land morphologies and accessibility conditions; thus, integrating regional difficulty coefficients or site-access cost parameters would enhance economic realism. Moreover, the assumption of a stationary wind regime does not account for long-term variations associated with climate change. Integrating meteorological time-series data, climate projections, and seasonal production variability would strengthen the environmental adaptability of the model. Finally, the assumption that the entire investment is financed through equity is inconsistent with typical real-world financing structures in both public and private sectors. Incorporating credit-based financing models, exchange-rate and interest-rate risks, and alternative repayment scenarios would significantly improve the model's economic applicability. Taken together, these potential enhancements underscore that the proposed model constitutes a flexible, extensible, and scientifically robust framework for sustainable regional energy planning.

ACKNOWLEDGEMENTS

This book was developed by expanding and revising a section of Selen AVCI AZKESKİN's doctoral dissertation titled "**Assessment of Renewable Energy Alternatives Based on Regional Energy Potential Through Clustering and Fuzzy Multi-Criteria Decision Making: A Site Selection Model for Wind Power Plants**" (**Thesis No: 970827**).

REFERENCES

Ackermann, T. (2005). *Wind power in power systems-transmission systems for offshore wind farms* (1st ed.). Stockholm, Sweden: John Wiley.

Arca, D., & Keskin Çıtıroğlu, H. (2020). GIS-based analysis of sites determination for wind power plant (WPP) by multi-criteria decision analysis: a case study in Yenice district (Karabük). *Karaelmas Science and Engineering Journal, 10*(2), 168-176.

Avcı Azkeskin, S., & Aladağ, Z. (2025). Evaluating regional sustainable energy potential through hierarchical clustering and machine learning. *Environmental Research Communications*, *7*(1), 015002.

Benti, N. E., Alemu, Y. B., Balta, M. M., Gunta, S., Chaka, M. D., Semie, A. G., . . . & Yohannes, H. (2023). Site suitability assessment for the development of wind power plant in wolaita area, southern ethiopia: an AHP-GIS model. *Scientific Reports, 13*(1), 19811.

Can, G., Kocabaldır, C., & Yücel, M. A. (2024). Spatial multi-criteria decision analysis for site selection of wind power plants: a case study. *Energy Sources, Part A: Recovery, Utilization, and Environmental Effects, 46*(1), 4012–4028.

Demir, G., Riaz, M., & Deveci, M. (2024). Wind farm site selection using geographic information system and fuzzy decision making model. *Expert Systems with Applications, 255*, 124772.

Denholm, P., Hand, M., Jackson, M., & Ong, S. (2009). Land-use requirements of modern wind power plants in the united states. *National Renewable Energy Laboratory*, Technical Report NREL/TP-6A2-45834.

Duval, G. (2025). *How Many Wind Turbines Can Fit on One Acre?* https://todayshomeowner.com/eco-friendly/guides/how-much-space-does-a-wind-turbine-need/.

World Health Organization (WHO) (2018). Environmental Noise Guidelines for the European Region. *WHO Regional Office For Europe*, Copenhagen, Denmark.

Ekiz, S., Şirin, A., & Erener, A. (2022). Determination of the most suitable wind power plant locations with geographical information systems: Kocaeli province example. *Journal of Geodesy and Geoinformation*, *9*(1), 59-79.

Elmahmoudi, F., Abra, O., Raihani, A., Serrar, O., & Bahatti, L. (2020). Elaboration of a wind energy potential map in Morocco using GIS and Analytic Hierarchy Process. *Engineering, Technology and Applied Science Research, 10*(4), 6068-6075.

Energy Atlas. (2025). *Installed Capacity of Power Plants, Electricity Generation and Consumption Data of Cities: Installed Capacity and Electricity Generation by Provinces.* https://www.enerjiatlasi.com/sehir/.

EPİAŞ. (2025). *Electricity Market Announcements*. https://www.epias.com.tr/tum-duyurular/01-07-2021-tarihinden-31-12-2025-tarihine-kadar-isletmeye-girecek-yek-belgeli-yenilenebilir-enerji-kaynaklarina-dayali-elektrik-uretim-tesisleri-icin-uygulanacak-guncellenmis-fiyatlar-hk-4/

Global Wind Atlas. (2024). *Wind Energy Layers.* https://globalwindatlas.info/en/

Hoang, T. N., Ly, T. B., & Do, H. T. (2022). A hybrid approach of wind farm site selection using group Best-Worst Method and GIS-based fuzzy logic relations: a case study in Vietnam. *Environmental Quality Management, 32*(3), 251-267.

Huang, X., Hayashi, K., & Fujii, M. (2023). Resources time footprint analysis of onshore wind turbines combined with GIS-Based site selection: a case study in fujian province, China. *Energy for Sustainable Development, 74*, 102-114.

International Renewable Energy Agency (IRENA). (2020). Renewable Power Generation Costs in 2019. *IRENA*, 46-56.

Kabak, M., & Taşkınöz, G. (2020). Determination of the installation sites of wind power plants with spatial analysis: a model proposal. *Sigma Journal of Engineering and Natural Sciences, 38*(1), 441–457.

Karipoğlu, F., Genç, M. S., & Koca, K. (2021). Determination of the most appropriate site selection of wind power plants based geographic information system and multi-criteria decision-making approach in Develi, Turkey. *International Journal of Sustainable Energy Planning and Management, 30,* 97-114.

Moradi, S., Yousefi , H., Noorollahi, Y., & Rosso, D. (2020). Multi-criteria decision support system for wind farm site selection and sensitivity analysis: case study of Alborz province, Iran. *Energy Strategy Reviews, 29*, 100478.

Onat, A., Alevli, B., & Kolay, M. (2016). Wind Power Plant (WPP) Preliminary Feasibility Report. *Republic of Türkiye Northern Anatolia Development Agency*, Report No: 2016-RP-7/103.

Oskay, C. (2014). The importance of wind energy within the sustainable development framework and the wind energy for investment incentives in Turkey. *Academic Review of Economics and Administrative Sciences*, *7*(1), 76.

Özşahin, E., & Kaymaz, Ç. K. (2013). A GIS analysis on the selection of the location of wind energy plant (WEP) installation: Sample of Hatay. *Journal of TUBAV Science*, *6*(2), 1-18.

Placide, G., & Lollchund, M. R. (2024). Wind farm site selection using GIS-based mathematical modeling and fuzzy logic tools: a case study of Burundi. *Frontiers in Energy Research, 12*, 1353388.

Rosas-Chavoya, M., Gallardo-Salazar, J. L., López-Serrano, P. M., Alcántara-Concepción, P. C., & León-Miranda, A. K. (2022). QGIS a constantly growing free and open-source geospatial software contributing to scientific development. *Cuadernos De Investigación Geográfica, 48*(1), 197-213.

Rossing, T. (2007). *Springer Handbook of Acoustics* (2nd ed.). New York: Springer NY.

Shorabeh, S. N., Firozjaei, H. K., Firozjaei, M. K., Jelokhani-Niaraki, M., Homaee, M., & Nematollahi, O. (2022). The site selection of wind energy power plant using GIS-multi-criteria evaluation from economic perspectives. *Renewable and Sustainable Energy Reviews, 168*, 112778.

Şahin, G., Koç, A., Doğan, S. Ş., Rustemli, S., & Sark, V. J. (2025). Exploring of wind energy potential and optimal site selection for wind energy plants installations in Erzurum/Turkey based on multicriteria site selection. *International Journal of Energy Research, 27*, 2629977.

Şentürk, A. E., & Oğuz, E. (2020). Environmental and economic analysis of onshore and offshore wind farms. *GMO Journal of Ship and Marine Technology*, *28*(217), 5-32.

T.C. Ministry of Energy and Natural Resources. (2022). Türkiye's Electricity Generation and Electricity Consumption Point Emission Factors. *Directorate of Energy Efficiency and Environment*, ETKB-EVÇED-FRM-042 Rev.01.

T.C. Ministry of Energy and Natural Resources. (2024). *Wind Energy Potential Atlas* (REPA). https://enerji.gov.tr/bilgi-merkezi-enerji-ruzgar.

Turkish Electricity Transmission Corporation (TEİAŞ). (2025). Türkiye Electricity Generation–Transmission Statistics for 2023. *Electricity Energy Generation–Consumption–Losses, Distribution of Türkiye's Electricity Generation by Sources in 2023.* https://www.teias.gov.tr/turkiye-elektrik-uretim-iletim-istatistikleri/

Tost, U., Akdeniz, E., & Kilvan, M. K. (2024). Mordoğan Wind Power Plant Real Estate Valuation Report. *Enda Energy Holding Co.*, Report No: 2023 / 1120.

URL-1: *USGS Earth Explorer.* https://earthexplorer.usgs.gov /.

URL-2: https://www.openstreetmap.org/#map=6/39.03/35.24/.

Uzar, M., & Şener, Z. (2019). Suitable map analysis for wind energy projects using remote sensing and GIS: a case study in Turkey. *Environmental Monitoring and Assessment, 191*(7), 459.

Vestas. (2025a). *2 Mw Platform Brochure.* https://www.vestas.com/content/dam/vestas-com/global/en/brochures/onshore/2mw_platform_brochure_.pdf.coredownload.inline.pdf/

Vestas. (2025b). *4 Mw Platform Brochure.* https://www.vestas.com/content/dam/vestas-com/global/en/brochures/onshore/4mw_platform_brochure.pdf.coredownload.inline.pdf/

Vestas. (2025c). *Enventus™ Platform Brochure.* https://www.vestas.com/en/energy-solutions/onshore-wind-turbines/enventus-platform/

Yaman, A. (2024). A GIS-based multi-criteria decision-making approach (GIS-MCDM) for determination of the most appropriate site selection of onshore wind farm in Adana, Turkey. *Clean Technologies and Environmental Policy, 26*, 4231–4254.

Yıldırım, H. H. (2017). Determination of payback periods in wind power generation investments by monte carlo simulation. *Istanbul Management Journal*, *28*(82), 76-104.

Yildiz, S. S. (2024). Spatial multi-criteria decision making approach for wind farm site selection: a case study in Balıkesir, Turkey. *Renewable and Sustainable Energy Reviews, 192*, 114158.

Yousefi, H., Moradi, S., Zahedi, R., & Ranjbar, Z. (2024). Developed Analytic Hierarchy Process and multi criteria decision support system for wind farm site selection using GIS: A regional-scale application with environmental responsibility. *Energy Conversion and Management: X, 22*, 100594.

Yousefi, H., Motlagh, S. G., & Montazeri, M. (2022). Multi-criteria decision-making system for wind farm site-selection using geographic information system (GIS): Case study of Semnan province, Iran. *Sustainability, 14*(13), 7640.

GIS-BASED SITE SUITABILITY ANALYSIS AND MATHEMATICAL MODELING FOR WIND ENERGY PLANNING: AN INTEGRATED APPROACH